Szomolay, B., Liu, J., Brown, P., Clement, M., Llewellyn-Lacey, S., Dolton, G., Ekeruche-Makinde, J., Lissina, A., Schauenburg, A. J. A., Sewell, A. K., Burrows, S. R., Roederer, M., Price, D. A., Wooldridge, L., & van den Berg, H. A. (2016). Identification of human viral protein-derived ligands recognized by individual MHCI-restricted T-cell receptors. *Immunology and Cell Biology*, *94*(6), 573–582. https://doi.org/10.1038/icb.2016.12

Peer reviewed version

Link to published version (if available):
10.1038/icb.2016.12

Identification of human viral protein-derived ligands recognized by individual major histocompatibility complex class I (MHCI)-restricted T-cell receptors

Barbara Szomolay[1,2], Jie Liu[3], Paul E. Brown[1], John J. Miles[4], Mathew Clement[2], Sian Llewellyn-Lacey[2], Garry Dolton[2], Julia Ekeruche-Makinde[5], Anya Lissina[6], Andrea J. Schauenburg[2], Andrew K. Sewell[2], Scott R. Burrows[4], Mario Roederer[3], David A. Price[2,3], Linda Wooldridge[6,*], Hugo A. van den Berg[1,*]

[1] Mathematics Institute, University of Warwick, Coventry CV4 7AL, UK.

[2] Institute of Infection and Immunity, Cardiff University School of Medicine, Heath Park, Cardiff CF14 4XN, UK.

[3] Vaccine Research Center, National Institute of Allergy and Infectious Diseases, National Institutes of Health, Bethesda, MD 20892, USA.

[4] QIMR Berghofer Medical Research Institute, Brisbane 4029, Australia.

[5] Wright Fleming Wing, St Mary's Campus, Imperial College, London SW7 2AZ, UK.

[6] Faculty of Health Sciences, University of Bristol, Medical Sciences Building, Bristol BS8 1TD, UK.

Running title: Identifying natural CD8$^+$ T-cell agonists

Keywords: T-cell activation, T-cell crossreactivity, autoimmunity, cancer, alloreactivity, leukaemia, T-cell expansions, MHCI, T-cell receptor.

Corresponding author: L. Wooldridge

email: linda.wooldridge@bristol.ac.uk

*LW and HAB contributed equally to this manuscript.

Abstract

Evidence indicates that autoimmunity can be triggered by virus-specific $CD8^+$ T-cells that crossreact with self-derived peptide epitopes presented on the cell surface by major histocompatibility complex class I (MHCI) molecules. Identification of the associated viral pathogens is challenging because individual T-cell receptors (TCRs) can potentially recognize up to a million different peptides. Here, we generate peptide length-matched combinatorial peptide library (CPL) scan data for a panel of virus-specific $CD8^+$ T-cell clones spanning different restriction elements and a range of epitope lengths. CPL scan data drove a protein database search, restricted to viruses that infect humans. Peptide sequences were ranked in order of likelihood recognition. For all anti-viral $CD8^+$ T-cell clones examined, the index peptide was either the top-ranked sequence or ranked as one of the most likely sequences to be recognized. Thus, we demonstrate that anti-viral $CD8^+$ T-cell clones are highly focused on their index peptide sequence and that "CPL-driven database searching" can be used to identify the inciting virus-derived epitope for a given $CD8^+$ T-cell clone. Moreover, to augment access to CPL-driven database searching, we have created a publicly accessible webtool. Application of these methodologies in the clinical setting may clarify the role of viral pathogens in the etiology of autoimmune diseases.

Introduction

$CD8^+$ T-cells recognize antigens in the form of intracellular protein-derived peptide fragments (8–14 amino acids in length) presented on the cell surface by major histocompatibility complex class I (MHCI) molecules. Although this *modus operandi* enables the elimination of cancerous or infected cells, dysregulated $CD8^+$ T-cell immunity can have devastating consequences for the host. For example, it has been proposed that $CD8^+$ T-cells play a major role in the pathogenesis of common autoimmune diseases, such as type I diabetes,[1,2,3] multiple sclerosis,[4] and psoriasis,[5] where pathogen-derived peptide sequences are thought to drive the expansion of self-reactive T-cells capable of mediating autoimmune attack.[6,7] This theory is supported by findings that microbial peptides can induce experimental autoimmune disease in mouse models and that human autoantigen-specific T-cells can recognize numerous peptides, some of which are microbial in origin.[8,9] Moreover, in certain disease states, the presence of monoclonal/oligoclonal $CD8^+$ T-cell expansions with a late differentiation phenotype, sometimes referred to as large granular lymphocytes (LGLs), is suggestive of an exaggerated antigen-specific response.[10] $CD8^+$ T-LGL expansions are a characteristic feature of LGL leukemia[11,12,13] and can be triggered by certain drugs, notably protein tyrosine kinase inhibitors.[14,15] $CD8^+$ T-cell expansions are also observed in autoimmune diseases such as rheumatoid arthritis[16] and aplastic anaemia.[17] It is possible that viral antigens drive these pathogenic $CD8^+$ T-cell expansions, which subsequently crossreact with self-derived peptide-MHCI (pMHCI) molecules to precipitate clinical disease.

Although it is clear that $CD8^+$ T-cells play an important role in health and disease, relatively little is known about the microbial and self-derived ligands involved in these processes. This lack of knowledge can to a large extent be attributed to the complexity of the peptide repertoire recognized by individual T-cell receptors (TCRs). Estimates suggest that there are $\sim$ 25 million unique T-cell receptors in the human TCR repertoire,[18] each with the potential to recognize up to one million different MHC-bound peptides.[19,20] Such promiscuous recognition has been deemed essential for effective immunity, as a relatively limited repertoire of TCRs must provide adequate coverage against a vast array of different pMHCI molecules.[21] Indeed, a given TCR may not only interact productively with ligands similar to the index peptide that triggered the initial response, but also with ligands that are unrelated in sequence,[22]

indicating that effective characterization of the cognate ligand repertoire must take the entire peptide universe into account without bias. A promising approach that satisfies these *desiderata* is combinatorial peptide library (CPL) scanning which can be combined with biometrical analysis to identify naturally occurring ligands.[23,24]

Although the set of peptides recognized by an individual TCR can be vast, not all of these sequences will be present in the naturally occurring MHCI-presentable peptide repertoire. Novel approaches are therefore required to identify biologically relevant ligands. Ideally, such an approach should incorporate: (i) an assessment of peptide length specificity;[25] (ii) an unbiased framework applicable to all TCRs irrespective of specificity and MHCI restriction; (iii) rapid throughput for clinical applicability; and (iv) an accurate end point for the reliable classification of response-evoking ligands *in vivo*.

Here, we develop and validate a strategy to examine the peptide repertoire recognized by individual TCRs. Raw datasets from length-matched CPL scans were used to rank peptides occurring in curated databases of viral pathogen or human self origin. The predictive value of the scoring method was then validated by measuring functional sensitivity for a selection of peptides spanning a range of predicted agonist likelihood values. This approach enabled us to identify the original viral determinant for a $CD8^+$ T-cell response. We envisage that "CPL-driven database searching" will find clinical utility across a range of immune-mediated diseases with currently unknown antigenic triggers.

Results

Development and validation of an effective approach to identify natural ligands recognized by individual MHCI-restricted TCRs

Pathogenic $CD8^+$ T-cell expansions may originate as an initially protective response to a viral antigen that results in immune-mediated disease, caused by subsequent crossreactivity with a self-derived pMHCI molecule. The need therefore arises to identify viral ligands that trigger $CD8^+$ T-cell expansions of unknown specificity. To develop and validate an approach to this problem, we interrogated a $CD8^+$ T-cell clone (E7NLV) specific for the immunodominant

HLA A*0201-restricted human cytomegalovirus (HCMV) $pp65_{495-503}$ epitope `NLVPMVATV`; HCMV is a member of the herpesvirus family that has been implicated in the pathogenesis of common $CD8^+$ T-cell-mediated diseases.[26]

MHCI-restricted TCRs display an explicit preference for peptide length, as attested by the fact that screening with CPLs of non-preferred length elicits a minute number of positive responses, whereas screening with CPLs of the preferred length elicits responses at every peptide position, allowing the molecular recognition landscape for each individual TCR to be mapped in detail.[25] Accordingly, we scanned E7NLV with a nonamer CPL to determine the amino acid preferences across the peptide backbone. Multiple responses were observed at the majority of positions, indicative of a crossreactive TCR with a propensity for degenerate peptide recognition (Figure 1). Although CPL scan data can be used to perform BLAST or motif-based searches directly, these approaches generate peptide lists without quantifying the likelihood of recognition. We took an alternative approach that uses raw peptide length-matched CPL scan data to search large protein databases, producing lists of potential peptide agonists ranked in order of likelihood of recognition. This ranking was achieved by assigning an agonist likelihood score Λ, as defined by eqn (8), to each subsequence in a protein database comprising the majority of known viruses regardless of host tropism.

To validate the accuracy of this approach, thirty peptide sequences were chosen by uniform sampling without repetition such that their Λ-values spanned approximately six orders of magnitude. Sampling was implemented using the MATLAB `datasample` command; when there were five different peptides in each bin for a given order of magnitude, the sampling algorithm halted. The peptides were synthesized and a functional sensitivity assay was performed. Figure 2a shows the functional response of E7NLV to the thirty selected peptides. A broad range of recognition was observed, with 15 out of 30 peptides acting as good agonists and 6 out of 30 peptides acting as strong agonists (Figure 2a). The functional sensitivity of the clone for each peptide was expressed as $p\mathrm{EC}_{50}$, the common cologarithm of the 50%-efficacy concentration. Relative functional sensitivity ($\Delta p\mathrm{EC}_{50}$) was calculated by subtracting the $p\mathrm{EC}_{50}$ of the index peptide from the $p\mathrm{EC}_{50}$ of the given peptide (Figure 2b). We examined the statistical dependence between Λ and $\Delta p\mathrm{EC}_{50}$ for all thirty randomly chosen peptides using Spearman's rank correlation test. The correlation for the peptides shown in Figure 2c was 0.49, which is significant at the 2% level, and the corresponding linear regression of $\Delta p\mathrm{EC}_{50}$ on Λ was significant at the 1% level. These results demonstrate that CPL-driven database searching can

accurately identify peptide sequences recognized by individual TCRs.

CPL-driven database searching can identify viral ligands that initiate CD8$^+$ T-cell responses

We next assessed whether our approach could be used to identify the original viral ligand that drove the initial expansion of a given clonotype, independently of prior knowledge of this ligand or the identity of the infectious agent. For this purpose, we constructed a database containing all human viral pathogens as well as all zoonotic viruses capable of or suspected to be capable of infecting humans, to the best of our knowledge and judgement. Each of the 1,872,417 unique nonamer peptide sequences in this database of 10,733 distinct viral proteins was assigned a Λ-value according to eqn (8), with parameter values derived from a nonameric CPL-scan of clone E7NLV. These sequences were ranked by Λ, which represents the likelihood of recognition by this clone. The index peptide of E7NLV, `NLVPMVATV`, was found to be the top-ranked sequence, suggesting that CPL-driven database searching alone can suffice to identify the infectious agent (Figure 3 and Table S1A). We examined the functional response to a further nine top-ranking peptides. In addition to the index, which had been recovered without prior knowledge, five out of the further nine predicted peptides were capable of activating E7NLV, with three being strong agonists (Figure 3). Thus, CPL-driven database searching could select from a comprehensive database the pathogen-derived sequence that had driven the initial expansion of clone E7NLV, as well as crossreactive peptide ligands.

CPL-driven database searching can identify viral ligands recognized by EBV-specific CD8$^+$ T-cells

To extend the foregoing findings to other specificities, we examined a panel of Epstein-Barr virus (EBV)-specific CD8$^+$ T-cell clones. EBV has been implicated in the pathogenesis of autoimmune diseases such as multiple sclerosis[27]. Our knowledge regarding the role of this virus in such diseases would therefore be advanced by a method that can define antigen specificity within the associated CD8$^+$ T-cell clonal expansions[28]. We initially focused on clones SB16 and SB12, which are both specific for the immunodominant HLA A*0201-restricted BMFL1$_{280-288}$ epitope `GLCTLVAML` (Table 1).

A nonamer CPL scan of the SB16 clone revealed multiple hits across the peptide backbone with dominant responses at each position (Figures 4 and S1). The raw CPL scan data set was used to conduct a CPL-driven search of the human viral database. Table S1B lists the nonameric peptide sequences ranked as the twenty sequences most likely to be recognized out of a database of 1,872,417 different nonameric sequences. The index peptide sequence for this clone was found to have the largest Λ-value, consistent with the result obtained for E7NLV (Table S1A). We next performed a nonamer CPL scan with clone SB12 (Table 1). In contrast to the result obtained with SB16, we did not detect responses that rose substantially above background, except at position 8, where a response to methionine (M) was observed (Figure S2); these results were too scanty to permit a meaningful CPL-driven database search and suggest that SB12 is highly ligand-specific, recognizing only a small number of peptides. This characteristic may be shared with other anti-viral $CD8^+$ T-cells, as we observed a similar result with ALF3, a $CD8^+$ T-cell clone specific for the immunodominant HLA A*0201-restricted influenza A $M1_{58-66}$ epitope `GILGFVFTL` (Table 1 and Figure S3).

$CD8^+$ T-cells specific for longer epitopes play a major role in the response against EBV.[29] We therefore examined two well-characterized clones with different EBV-derived peptide length preferences. Clone SB14 is specific for the immunodominant HLA B*3508-restricted $EBNA1_{407-417}$ epitope `HPVGEADYFEY` (Table 1) and we therefore performed an 11-mer CPL scan on this clone (Figures 4 and S4). A CPL-driven search of the human viral database predicted that the two most likely recognized 11-mer peptide sequences were `HPVAEADYFEY` and `HPVGDADYFEY` (4A and 5D variants of the index peptide), with the index peptide itself ranking third in the list (Table S1C). Clone SB27 is specific for the HLA B*3508-restricted $BZFL1_{52-64}$ epitope `LPEPLPQGQLTAY` and exhibits a strong preference for 13-mer peptides.[25] A 13-mer CPL scan of this clone revealed a high degree of crossreactivity (Ekeruche-Makinde *et al.*[25], and Figure 4), but notwithstanding this apparent promiscuity, the index peptide still ranked twelfth in a CPL-driven search of the human viral database (Table S1D).

Collectively, these findings demonstrate that viral peptide specificities can be identified efficiently by means of peptide length-matched CPL-driven database searching. In general, anti-viral $CD8^+$ T-cells appear to be highly focused on their index peptide sequence, notwithstanding an inherent degree of crossreactivity.

CPL-driven database searching can identify variants recognized by HIV-1-specific CD8$^+$ T-cells

To examine the utility of CPL-driven database searching in other viral infections, we studied two previously described TCRs specific for the immunodominant human immunodeficiency virus type 1 (HIV-1)-derived HLA A*0201-restricted p17 Gag_{77-85} epitope SLYNTVATL (Table 1). Consistent with the results above, a CPL-driven search of the human viral database using nonamer CPL scan data from the 003 clone identified the index sequence as the most likely agonist (Figures 4 and S5; Table S1E). Moreover, a number of epitope variants were predicted, many of which have been verified at the functional level.[30,31] Similar results were obtained with the 868 TCR, in this case scanning primary CD8$^+$ T-cells transduced with the corresponding lentiviral construct (Figures 4 and S6; Table S1F). CPL-driven database searching can therefore predict epitope variant crossreactivity patterns, which may prove useful in the assessment of CD8$^+$ T-cell responses against highly variable viruses.

Extending the approach to the identification of self ligands targeted by CD8$^+$ T-cells

In addition to the identification of virus-derived epitopes, it would be advantageous if CPL-driven database searching could reveal self-derived peptide targets, as this would provide a means to identify the antigenic proteins involved in autoimmune disease and, moreover, to discover novel cancer epitopes recognized by CD8$^+$ T-cells. To this end, we created a human protein database as described below. The CD8$^+$ T-cell clones ILA1 and MEL5 were chosen because they are both specific for epitopes derived from self proteins. In particular, ILA1 is specific for the HLA A*0201-restricted human telomerase reverse transcriptase $(hTERT)_{540-548}$ sequence ILAKFLHWL (Table 1). A nonamer CPL scan previously carried out for ILA1[25,32] was used to conduct a CPL-driven search of the human protein database (Figure 4). The index peptide was ranked by Λ as the eighth most likely nonameric peptide sequence to be recognized by the ILA1 TCR, suggesting that this approach is capable of identifying self-derived ligands targeted by TCRs (Table S2A).

However, a previous study indicated that ILAKFLHWL is not expressed at the cell surface[33], and therefore ILA1 may not be typical of a self-reactive TCR that has survived negative selection. To address this potential confounder, we

studied MEL5, which recognizes the HLA A*0201-restricted Melan-A/MART1 epitope EAAGIGILTV.[34] A nonamer CPL scan, which had previously been carried out for MEL5,[25,34] was used to conduct a CPL-driven search of the human protein database (Figure 4). The EAAGIGILTV peptide sequence did not appear in the top twenty peptides predicted to activate MEL5 (EAAGIGILTV ranked 55th; Table S2B). Self-reactive TCRs are possibly not focused on their index peptide sequence to the same degree as virus-specific TCRs and, consequently, the CPL-driven database searching approach may fail to identify disease-relevant ligands targeted by self-reactive TCRs. The use of smaller disease-specific or organ-specific databases might improve the applicability of our strategy in this context.

Overview of CPL-driven database screening and development of a webtool

Every TCR is characterized by a unique peptide recognition signature, which comprises three different components: (i) a peptide length preference; (ii) the number of peptides recognized at this preferred length; and (iii) the sequence identity of these peptide agonists, which may be either pathogen-derived or self-derived.[20,25] Figure 5 provides an overview of a three-stage strategy to dissect the peptide recognition signature of a given TCR. In the first stage, peptide length preference is determined by examining functional recognition of a "sizing scan" comprising random peptide libraries of different lengths (x_8, x_9, x_{10}, x_{11}, x_{12}, x_{13}, where x denotes any of the 19 L-amino acids excluding cysteine).[25] In the second stage, CPL-biased sampling[19] is used to quantify the number of recognized peptides. In the third stage, which is the novel step introduced in the present study, CPL-driven database searching is used to identify antigen specificity. To augment community-wide access to CPL-driven database searching, we created a dedicated webtool as part of the WSBC webtools framework.

Discussion

Although $CD8^+$ T-cells protect the human body from countless intracellular pathogens and malignant processes, they are also heavily implicated in the etiology of life-threatening and incurable immune-mediated diseases. It is

conceivable that non-self antigens elicit $CD8^+$ T-cell responses that are initially target-appropriate but subsequently become pathogenic as a consequence of crossreactivity with self epitopes. In this study, we developed and validated a technique termed "CPL-driven database searching", which allows for the reliable identification of cognate viral epitopes recognized by $CD8^+$ T-cells with as yet unknown specificities. Initially, we constructed a viral database containing human and zoonotic viruses (with an established or potential ability to infect humans). This database was curated to include non-redundant and reviewed sequences only and contained a total of 10,733 viral proteins. We then selected a panel of herpesvirus-specific $CD8^+$ T-cell clones spanning two different restriction elements (HLA A*0201 and HLA B*3508) and a range of epitope lengths (9–13 amino acids). As $CD8^+$ T-cells typically display an explicit preference for peptide length,[25] we focused our attention on peptide length-matched CPL scans to determine the amino acid preferences of each clone at each peptide position. The majority of clones in our panel elicited strong responses with distinct preference hierarchies at each position of the peptide. CPL scan datasets were used to assign an agonist likelihood score (Λ) to each peptide of preferred length in the entire human viral database, thereby producing a list of potential peptide ligands in order of likelihood of recognition. For all herpesvirus-specific clones tested, the index epitope ranked in the top-twenty most likely recognized peptide sequences from the entire human viral database, even for the highly crossreactive $CD8^+$ T-cell clone SB27, which is specific for an HLA B*3508-restricted 13-mer EBV-derived epitope. These findings indicate that anti-viral $CD8^+$ T-cells display high levels of functional sensitivity for the index epitope, consistent with an efficient *in vivo* selection process based on interclonal competition for antigen.[35]

It is noteworthy that one EBV-specific $CD8^+$ T-cell clone tested failed to respond to any CPL scan mixtures except mixture M@8 and was not suitable for further analysis. This difficulty could be emblematic of a small subset of $CD8^+$ T-cell clones that are highly focused on the salient ligand and therefore fail to respond to a sufficiently large number of peptides within the CPL mixtures. CPL-driven database searching is not applicable to such TCRs, which behave as "non-responders" in the context of a CPL scan. Moreover, to ensure the accuracy of CPL-driven database searching, experimental $CD8^+$ T-cell populations must be monoclonal and must be subjected to multiple replicates of each scan.

The viral pathogen and human proteome databases were collated and curated with a view to making them as

exhaustive as possible. It may be considered that the relatively small size of the former database contributes to the success of our method, but this is not the case. Indeed, when the two databases were merged, comparable rankings were obtained. In terms of *relative rank*, the merged database was slightly better for most TCRs, indicating that the ranks derived from the viral database are actually more conservative. Notwithstanding these advantages, the identification of relevant epitopes in the human proteome database is much more challenging, likely due to the fact that even physiologically relevant autoimmune epitopes are typically recognized at low levels of functional sensitivity. Work is in progress to build and test similar databases for bacterial and fungal pathogens. These will be added to the webtool on completion.

It is known that HIV-1 can escape from the $CD8^+$ T-cell response via single point mutations in key epitopes.[36] If $CD8^+$ T-cells are inherently crossreactive, why does the HIV-1-specific $CD8^+$ T-cell response exhibit such exquisite specificity? Our findings point to a possible explanation. The HIV-1-specific TCRs examined in this study (003 and 868) were strongly focused on their index peptide sequence, increasing the probability that epitope mutation will result in loss of recognition. In contrast, $CD8^+$ T-cells with a more crossreactive phenotype are associated with delayed disease progression.[37,38] It is therefore feasible that CPL-driven database searching will provide a useful tool to delineate the requirements for effective $CD8^+$ T-cell-mediated immunity against HIV-1.

CPL-driven database searching may also assist in the identification of self-derived epitopes, such as those targeted by autoimmune or cancer-specific $CD8^+$ T-cells. Indeed, similar approaches to ligand hunting in these settings have been described previously.[39,40] Although we successfully identified the index peptide for the ILA1 clone, it has been shown that the cognate epitope is not expressed on the surface of HLA A*0201$^+$ hTERT$^+$ cancer cell lines,[33] which renders it less likely that this epitope is expressed in the thymus. If so, ILA1 will not have been subjected to negative selection in the thymus, which could account for the highly focused phenotype of this clone. In contrast, the index `EAAGIGILTV` peptide recognized by the MEL5 clone was ranked at position 55. It may therefore be more challenging to identify *bona fide* self-derived epitopes that are expressed in the thymus. Generation of disease-specific or organ-specific protein databases might circumvent this problem by narrowing the search for relevant epitopes, but further work is required to test such focused screening strategies.

In summary, we have developed and validated an approach that can be used to dissect the peptide recognition signature of any given TCR. Accordingly, we therefore anticipate that CPL-driven database searching will find clinical utility across a range of diseases.

Methods

Cells

Ten human $CD8^+$ T-cell clones spanning eight different specificities were used in this study (Table 1). The index peptides for the following $CD8^+$ T-cell clones are derived from viral proteins; E7NLV, SB16, SB12, ALF3,[41] SB14,[42] SB27,[43] 003[44] and 868.[44] The index peptides for the remaining two $CD8^+$ T-cell clones, ILA1[45] and MEL5,[46] are derived from human self proteins. Clone E7NLV is specific for the HLA A*0201-restricted HCMV-derived pp65 epitope `NLVPMVATV` (residues 495–503). Four clones are specific for epitopes derived from EBV proteins: SB16 and SB12, which both recognize the HLA A*0201-restricted BMLF1 epitope `GLCTLVAML` (residues 280–288); SB14, which recognizes the HLA B*3508-restricted EBNA1 epitope `HPVGEADYFEY` (residues 407–417); and SB27, which recognizes the HLA B*3508-restricted BZLF1 epitope `LPEPLPQGQLTAY` (residues 52–64). Clone ALF3 is specific for the HLA A*0201-restricted influenza A-derived M1 epitope `GILGFVFTL` (residues 58–66; Clement *et al.*[41]). The 003 and 868 TCRs are both specific for the HLA A*0201-restricted HIV-1-derived p17 Gag epitope SLYNTVATL (residues 77–85). Clone ILA1 is specific for the HLA A*0201-restricted hTERT-derived sequence `ILAKFLHWL` (residues 540–548), and clone MEL5 is specific for the Melan-A-derived heteroclitic sequence `ELAGIGILTV` (residues 26–35). All $CD8^+$ T-cells were maintained in RPMI 1640 containing 100 U/ml penicillin, 100 mg/ml streptomycin, 2 mM L-glutamine and 10% heat-inactivated fetal calf serum (all Life Technologies), supplemented with 2.5% Cellkines (Helvetica Healthcare), 200 IU/ml interleukin IL-2 and 25 ng/ml IL-15 (both PeproTech). C1R-HLA A*0201 and T2-HLA B*3508 target cells were generated and maintained as described previously.[47]

Combinatorial peptide library scans

CPL libraries were synthesized in a positional scanning format (Pepscan Presto^{Ltd}). All CPL scans were performed as previously described.[19,25,32] Briefly, 6×10^4 target cells were incubated with various library mixtures (at 100 μM) in duplicate for 2 hours at 37°C. After peptide pulsing, 3×10^4 clonal CD8$^+$ T-cells were added and the plates were incubated overnight to 37°C. Supernatants were then collected and assayed for MIP1β content by ELISA (R&D Systems).

Functional sensitivity assays

For MIP1β ELISA assays, 6×10^4 target cells were pulsed with peptide at the indicated concentrations for 2 hours at 37°C. Subsequently, 3×10^4 clonal CD8$^+$ T-cells were added and the plates were incubated overnight at 37°C. Supernatants were then collected and assayed for MIP1β by ELISA (R&D Systems). For lysis assays, target cells were loaded with ^{51}Cr for 1 hour and then plated at 5,000 cells per well in 75 μl medium. Clonal CD8$^+$ T-cells were added to a total volume of 150 μl. Target cells alone were to used to measure spontaneous release and Triton 100 was used to measure total release. After incubation for 4 hours at 37°C, 15 μl supernatant per well was harvested and mixed with 150 μl OptiPhaseSupermix Scintillation Cocktail (Perkin-Elmer). Release of ^{51}Cr was measured with a Microbeta Counter (Wallac) and the resulting data were used to calculate % specific lysis according to the formula:

$$\frac{\text{Experimental release} - \text{spontaneous release}}{\text{Total release} - \text{spontaneous release}} \times 100\%$$

Functional sensitivity was determined as described previously;[19] it is expressed as $p\text{EC}_{50}$, the cologarithm to base 10 of the 50%-efficacy concentration as determined from dose-response experiments in which antigen-presenting cells were incubated with agonist across a series of dilutions.

Derivation of the agonist likelihood score method

The functional sensitivity of a clone of interest to a given peptide ligand depends on several factors, a key parameter being the rate at which a single peptide-MHC copy elicits TCR triggering.[48,49] We quantify TCR degeneracy as the probability that the functional sensitivity of a given TCR to a randomly chosen ligand exceeds a given value ω;[50] this probability expresses the degeneracy at ω. Let w_{ij} denote the functional sensitivity of TCR i to peptide j, where $w_{ij} \leq \widehat{w}$ for all i and j (with $\widehat{w} > 0$). Besides being a function of clonotype i and peptide-MHCI species j, functional sensitivity depends on additional factors such as phenotypic differentiation stage and coreceptor expression; we assume such additional parameters to be uniform across the experiments performed in the present study. If n is the length of the peptides considered, then 20^n is the size of the peptide universe (the total number of distinct peptides). Given a peptide subset $\mathscr{S}$ of the peptide universe, the general question of epitope prediction can be framed as follows: for a clone of interest i, determine the quantity $\mathbb{P}[w_{ij} > \omega | j \in \mathscr{S}]$, i.e. the probability that w_{ij} exceeds a set value $\omega \in [0, \widehat{w}]$, when it is known that the peptide ligand j belongs to this set $\mathscr{S}$. For a peptide j selected at random, we have $\mathbb{P}[j \in \mathscr{S}] = 20^{-n}|\mathscr{S}|$, where $|\mathscr{S}|$ denotes the cardinality of $\mathscr{S}$. Then, by Bayes' Rule,

$$\mathbb{P}[w_{ij} > \omega | j \in \mathscr{S}] = \mathbb{P}[j \in \mathscr{S} | w_{ij} > \omega] \frac{\mathbb{P}[w_{ij} > \omega]}{\mathbb{P}[j \in \mathscr{S}]} = \mathbb{P}[j \in \mathscr{S} | w_{ij} > \omega] \, \mathbb{P}[w_{ij} > \omega] 20^n |\mathscr{S}|^{-1} \, , \tag{1}$$

which expresses the problem in the empirically more accessible probability $\mathbb{P}[j \in \mathscr{S} | w_{ij} > \omega]$, i.e. the chance that a randomly selected peptide j belongs to $\mathscr{S}$, given that the functional sensitivity w_{ij} to this peptide is at least ω. A direct estimate of this probability could be obtained by subjecting randomly generated peptides to a functional sensitivity assay and verifying whether they also belong to $\mathscr{S}$. However, this would be highly inefficient and would require millions of random peptides to be reasonably accurate, as the vast majority would be practically "null" (i.e. having $p\mathrm{EC}_{50}$ well below the detection limit). More progress can be made provided that $\mathscr{S}$ is a cylinder, which is a special type of set, defined as follows: let $1 \leq p_1 < p_2 < ... < p_k \leq n$ represent a choice of positions in the peptide and let $\alpha_1, \alpha_2, ..., \alpha_k$ be a choice of amino acid residues for these positions (several or all of these αs could be the same amino

acid). Then a peptide set of the form

$$\mathscr{C}^{p_1,\ldots,p_k}_{\alpha_1,\ldots,\alpha_k} = \{ \text{ peptides such that the residue at position } \ p_r \ \text{ is } \ \alpha_r \ \text{ for } \ r = 1,\ldots,k\}$$

is called a *cylinder of rank k*. For example, the rank-2 cylinder $\mathscr{C}^{4,5}_{\mathrm{Q,R}}$ contains all and only the peptides with glutamine at position 4 and arginine at position 5. The cardinality of a rank-k cylinder is 20^{n-k}; in particular, the rank-0 cylinder is the entire peptide universe, as no amino acids are specified at any position, whereas a rank-n cylinder contains just one peptide, all positions having been specified.

Given a rank-k cylinder $\mathscr{C}^{p_1,\ldots,p_k}_{\alpha_1,\ldots,\alpha_k}$, let $\mathbb{J}$ denote a subset of $\{p_1,\ldots,p_k\}$, and let $\mathscr{C}^{\mathbb{J}}_{\alpha[\mathbb{J}]}$ be the lower-order cylinder which has amino acids specified only at the positions in $\mathbb{J}$, agreeing with the 'parent' $\mathscr{C}^{p_1,\ldots,p_k}_{\alpha_1,\ldots,\alpha_k}$ at those positions, that is, $\mathscr{C}^{\mathbb{J}}_{\alpha[\mathbb{J}]}$ is formed by dropping from $\mathscr{C}^{p_1,\ldots,p_k}_{\alpha_1,\ldots,\alpha_k}$ the positions not present in $\mathbb{J}$. Let ℓ be an integer $0 \le \ell \le k$, and let $\binom{\{p_1,\ldots,p_k\}}{\ell}$ denote the set of all subsets $\mathbb{J}$ of size ℓ, so that cylinders can be decomposed as follows:

$$\mathscr{C}^{p_1,\ldots,p_k}_{\alpha_1,\ldots,\alpha_k} = \bigcup_{\mathbb{J}\in\binom{\{p_1,\ldots,p_k\}}{k-1}} \mathscr{C}^{\mathbb{J}}_{\alpha[\mathbb{J}]}. \tag{2}$$

Next, let correlation functions be defined recursively, as follows:

$$K^{p_1,\ldots,p_k}_{\alpha_1,\ldots,\alpha_k}(\omega;i) = \frac{20^k\,\mathbb{P}[j \in \mathscr{C}^{p_1,\ldots,p_k}_{\alpha_1,\ldots,\alpha_k} \mid w_{ij} > \omega]}{\prod_{\ell=0}^{k-1}\prod_{\mathbb{J}\in\binom{\{p_1,\ldots,p_k\}}{\ell}} K^{\mathbb{J}}_{\alpha[\mathbb{J}]}(\omega;i)} \tag{3}$$

with lowest-order boundary condition $K^{\emptyset}_{\emptyset}(\omega,i) \equiv 1$ for all $\omega \in [0,\widehat{w}]$. The correlation functions permit an *exact* solution of the epitope prediction problem, since eqn (3) implies that

$$\mathbb{P}[j \in \mathscr{C}^{p_1,\ldots,p_k}_{\alpha_1,\ldots,\alpha_k} \mid w_{ij} > \omega] = 20^{-k}\prod_{\ell=1}^{k}\prod_{\mathbb{J}\in\binom{\{p_1,\ldots,p_k\}}{\ell}} K^{\mathbb{J}}_{\alpha[\mathbb{J}]}(\omega;i) \tag{4}$$

and with eqn (1) this can be transformed into the probability that a peptide is an agonist with functional sensitivity of at least ω, given that the peptide belongs to some cylinder of interest, which might be of appropriate cardinality, be this almost the entire peptide universe or a singleton set (i.e. a rank-n cylinder containing only that peptide).

The crucial step is to establish a connection to CPL data. Consider the CPL mixture K@3, in which lysine is fixed at position 3 with all other positions random. This mixture corresponds to the rank-1 cylinder $\mathscr{C}^3_{\mathrm{K}}$. Similar correspondences obtain for all 180 CPL mixtures (in the case $n = 9$). Suppose that a peptide contributes appreciably to the CPL read-out whenever w_{ij} exceeds a certain cut-off value $\widetilde{\omega}$, let $Y^{\alpha}_{p}(i)$ denote the read-out signal obtained when exposing clone i to the mixture $\alpha@p$, and let $\mathscr{A}$ denote the set of 20 amino acids. We then propose the following identification:

$$\mathbb{P}[j \in \mathscr{C}^{p}_{\alpha} \mid w_{ij} > \widetilde{\omega}] = \frac{Y^{\alpha}_{p}(i)}{\sum_{\alpha' \in \mathscr{A}} Y^{\alpha'}_{p}(i)} \tag{5}$$

where p is the single specified position (with $1 \leq p \leq n$) and α is the specified amino acid residue at this position. The rank-1 specialisation of eqn (3) is as follows:

$$\mathbb{P}[j \in \mathscr{C}^{p}_{\alpha} \mid w_{ij} > \omega] = \frac{1}{20} K^{p}_{\alpha}(\omega; i) \tag{6}$$

and thus, with ω set to $\widetilde{\omega}$, eqn (5) provides a way to estimate the lowest-order correlation function from the CPL scan data. The proposed identification, eqn (5), rests on somewhat idealised assumptions, since peptides with values with w_{ij} below $\widetilde{\omega}$ may still contribute if they are presented at high copy numbers on the antigen-presenting cell and conversely, peptides with high w_{ij} may fail to contribute substantially.

In principle, higher-rank correlation functions can be estimated from higher-rank CPLs, which contain library mixtures corresponding to higher-rank cylinders (e.g. the mixture K@3&A@5 corresponds to the rank-2 cylinder $\mathscr{C}^{3,5}_{\mathrm{K,A}}$), but the number of peptide mixtures required, and hence the cost of the experiment, quickly becomes prohibitive.

Rank-1 correlations can nevertheless be informative as long as that higher-order correlations do not dominate. Mathematically speaking, the higher-order correlations are neglected by setting the corresponding K-values equal to 1; this amounts to a truncation of the exact expansion in eqn (4). Combining eqns (1) and (5) with the truncated version of eqn (4), we obtain the following for a specified peptide $\alpha_1\alpha_2\cdots\alpha_n$:

$$\ln \mathbb{P}[w_{ij} > \widetilde{\omega} \mid \text{peptide } j \text{ is } \alpha_1\alpha_2\cdots\alpha_n] \approx \ln P_i(\widetilde{\omega}) + n\ln\{20\} + \sum_{p=1}^{n} \ln \frac{Y_p^{\alpha_p}(i)}{\sum_{\alpha'\in\mathscr{A}} Y_p^{\alpha'}(i)} \tag{7}$$

where $P_i(\widetilde{\omega})$ is the unconditional probability that the functional sensitivity of clone i for a peptide selected at random exceeds $\widetilde{\omega}$. For the purpose of ranking peptides, we can proceed without knowing the value of $P_i(\widetilde{\omega})$, since it merely represents a fixed offset term, once a clone has been fixed. We therefore retain only the last term in eqn (7), which we call the *agonist likelihood score*:

$$\Lambda(\alpha_1\alpha_2\cdots\alpha_n; i) = \sum_{p=1}^{n} \ln \frac{Y_p^{\alpha_p}(i)}{\sum_{\alpha'\in\mathscr{A}} Y_p^{\alpha'}(i)} \ . \tag{8}$$

MATLAB scripts were written to scan the human and viral pathogen databases and to evaluate Λ for all potential peptides of the clone-appropriate length in the proteomes, i.e. all subsequences of the specified length irrespective of antigen processing constraints. Excluded were those containing one or more unspecified residues, appearing as `X` in the databases; such cases were rare. NetChop predictions of MHCI binding were also obtained via the publicly available online tool, but these data are not reported here because we did not find that they winnowed the candidate peptide list.

Data access provisions

Databases

Human and viral databases were compiled on the basis of publicly available protein sequence databases provided by NCBI (National Center for Biotechnology Information), UniProt (Universal Protein Resource), and PDB (Protein Data Bank). The human proteome database was assembled using protein sequence information taken from the following data sources:

(i) file `protein.fa.gz` from

`ftp://ftp.ncbi.nih.gov/genomes/Homo_sapiens/protein/`;

(ii) file `human.protein.faa.gz` from

`ftp://ftp.ncbi.nih.gov/refseq/H_sapiens/mRNA_Prot/`;

(iii) `http://www.uniprot.org/uniprot/` for canonical and isoform sequence data in FASTA format (Protein Knowledgebase search terms: *organism:homo sapiens* and *reviewed:yes*);

(iv) `http://www.pdb.org/pdb/home/home.do` for human protein sequences

(search terms: *taxonomy:homo sapiens*, *polymer type:protein*, *custom tabular report:sequence*, *macromolecular name*, *source*).

The viral protein database was assembled using protein sequence information taken from the following data sources:

(i) file `viral.1.protein.faa.gz` from

`ftp://ftp.ncbi.nih.gov/refseq/release/viral/`;

(ii) file `all.faa.tar.gz` from

ftp://ftp.ncbi.nih.gov/genomes/Viruses;

(iii) http://www.uniprot.org/uniprot/ for canonical and isoform sequence data in FASTA format (Protein Knowledgebase search terms: *host:human* and *reviewed:yes*);

(iv) http://www.pdb.org/pdb/home/home.do for viral protein sequences

(search terms: *taxonomy:viruses*, *polymer type:protein*, *custom tabular report:sequence, macromolecular name, source*).

(Remote file names and locations may be subject to change.) The assembled databases were curated to contain non-redundant and certified sequences, comprising 54,886 human and 187,840 viral proteins, respectively. As the viral database was compiled from a variety of data sources, care was taken to ensure that each pathogen was identified by a unique key and that different keys for the same pathogen used in different sources were slaved to the master key. A list of approximately 250 viral species with known or potential ability to infect humans was compiled and used to restrict the viral database to pathogens that infect humans; avoidance of ambiguity poses a major challenge in the face of issues surrounding the distinction of closely related species of viral pathogens and the frequent use of alternative designations. Ultimately, there were 10,733 non-redundant protein sequences in the database of proteomes of viral pathogens that pose a potential danger to human beings.

Webtool

A novel webtool, PI CPL, was written in MATLAB and compiled using the MATLAB Compiler. The binary code was integrated into the WSBC webtools framework, accessible at

http://wsbc.warwick.ac.uk/wsbcToolsWebpage.

The framework provides a browser-based user interface, from which jobs are launched and run on a multicore computational cluster. Feedback on progress is provided via a webpage if required. Results are presented as a webpage and can also be downloaded for offline viewing. In the case of PI CPL, these consist of a text file containing a list of the top-scoring peptides, which is designed to be viewed as a spreadsheet, plus a heat map image. A database of results is maintained as a job history for logged-on users. To request an account, please email the corresponding author.

Acknowledgements

We thank Professor Rodney Phillips for provision of clone 003. This work was supported by the Biotechnology and Biological Sciences Research Council (Grant BB/H001085/1) and the Wellcome Trust (WT079848MA). D. A. P. and A. K. S. are Wellcome Trust Investigators.

Conflict of interest

The authors declare no conflicts of interest.

References

[1] Skowera A, Elps R, Varela-Calviño R, Arif S, Huang G, Van-Krinks C *et al.* CTLs are targeted to kill beta cells in patients with type 1 diabetes through recognition of a glucose-regulated preproinsulin epitope. *J Clin Invest* 2008; **118**: 3390–3402.

[2] Kronenberg D, Knight RR, Estorninho M, Ellis RJ, Kester MG, de Ru A *et al.* Circulating preproinsulin signal peptide-specific CD8 T cells restricted by the susceptibility molecule HLA-A24 are expanded at onset of type 1 diabetes and kill β-cells. *Diabetes* 2012; **61**: 1752–1759.

[3] Coppieters KT, Dotta F, Amirian N, Campbell PD, Kay TW, Atkinson MA *et al.* Demonstration of islet-autoreactive CD8 T cells in insulitic lesions from recent onset and long-term type 1 diabetes patients. *J Exp Med* 2012; **209**: 51–60.

[4] Friese MA Fugger L. Pathogenic cells $CD8^+$ T in multiple sclerosis. *Ann Neurol* 2009; **66**: 132–141.

[5] Diani M, Altomare G Reali E. T cell responses in psoriasis and psoriatic arthritis. *Autoimmun Rev* 2014; **14**: 286–292.

[6] Selin LK, Wlodarczyk MF, Kraft AR, Nie S, Kenney LL, Puzone R *et al.* Heterologous immunity: Immunopathology, autoimmunity and protection during viral infections. *Autoimmunity* 2011; **44**: 328–347.

[7] Coppieters KT, Wiberg A von Herrath MG. Viral infections and molecular mimicry in type 1 diabetes. *APMIS* 2012; **120**: 941–949.

[8] Wucherpfennig KW Strominger JL. Molecular mimicry in T cell-mediated autoimmunity: Viral peptides activate human T cell clones specific for myelin basic protein. *Cell* 1995; **80**: 695–705.

[9] Hemmer B, Fleckenstein BT, Vergelli M, Jung G, McFarland H, Martin R *et al.* Identification of high potency

microbial and self ligands for a human autoreactive class II-restricted T cell clone. *J Exp Med* 1997; **185**: 1651–1659.

[10] Rodríguez-Caballero A, García-Montero AC, Bárcena P, Almeida J, Ruiz-Cabello F, Tabernero MD *et al.* Expanded cells in monoclonal TCR-$\alpha\beta^{+}$/CD4^{+}/NKa/CD8$^{+/-\mathrm{dim}}$ T-LGL lymphocytosis recognize hCMV antigens. *Blood* 2008; **112**: 4609–4616.

[11] Melenhorst JJ, Brummendorf TH, Kirby M, Lansdorp PM Barrett AJ. CD8+ T cells in large granular lymphocyte leukemia are not defective in activation- and replication-related apoptosis. *Leuk Res* 2001; **25**: 699–708.

[12] Melenhorst JJ, Sorbara L, Kirby M, Hensel NF Barrett AJ. Large granular lymphocyte leukaemia is characterized by a clonal T-cell receptor rearrangement in both memory and effector CD8(+) lymphocyte populations. *Br J Haematol* 2001; **112**: 189–194.

[13] Melenhorst JJ, Eniafe R, Follmann D, Molldrem J, Kirby M, Ouriaghli FE *et al.* T-cell large granular lymphocyte leukemia is characterized by massive TCRBV-restricted clonal CD8 expansion and a generalized overexpression of the effector cell marker CD5. *J Hematol* 2003; **4**: 18–25.

[14] Mustjoki S, Ekblom M, Arstila TP, Dybedal, Epling-Burnette PK, Guilhot F *et al.* Clonal expansion of T/NK-cells during tyrosine kinase inhibitor dasatinib therapy. *Leukemia* 2009; **23**: 1398–1405.

[15] Kreutzman A, Ladell K, Koechel C, Gostick E, Ekblom M, Stenke L *et al.* Expansion of highly differentiated

CD8+ T-cells or NK-cells in patients treated with dasatinib is associated with cytomegalovirus reactivation. *Leukemia* 2011; **25**: 1587–1597.

[16] Gonzalez-Quintial R, Baccala R, Pope RM Theofilopoulos AN. Identification of clonally expanded T cells in rheumatoid arthritis using a sequence enrichment nuclease assay. *J Clin Invest* 1996; **97**: 1335–1343.

[17] Risitano AM, Kook H, Zeng W, Chen G, Young NS Maciejewski JP. Oligoclonal and polyclonal CD4 and CD8 lymphocytes in aplastic anemia and paroxysmal nocturnal hemoglobinuria measured by V beta CDR3 spectratyping and flow cytometry. *Blood* 2002; **100**: 178–183.

[18] Arstila TP, Casrouge A, Baron V, Even J, Kanellopoulos J Kourilsky P. A direct estimate of the human alpha beta T cell receptor diversity. *Science* 1999; **286**: 958–961.

[19] Wooldridge L, Ekeruche-Makinde J, van den Berg HA, Skowera A, Miles JJ, Tan MP *et al.* A single autoimmune T cell receptor recognizes more than a million different peptides. *J Biol Chem* 2012; **287**: 1168–1177.

[20] Wooldridge L. Individual MHCI-restricted T-cell receptors are characterized by a unique peptide recognition signature. *Front Immunol* 2013; **4:199**.

[21] Mason D. A very high level of crossreactivity is an essential feature of the T-cell receptor. *Immunol Today* 1998; **19**: 395 – 404.

[22] Ignatowicz L, Rees W, Pacholczyk R, Ignatowicz H, Kushnir E, Kappler J *et al.* T cells can be activated by peptides that are unrelated in sequence to their selecting peptide. *Immunity* 1997; **7**: 179–186.

[23] Pinilla C, Martin R, Gran B, Appel JR, Boggiano C, Wilson DB *et al.* Exploring immunological specificity using synthetic peptide combinatorial libraries. *Curr Opin Immunol* 1999; **11**: 193–202.

[24] Nino-Vasquez JJ, Allicotti G, Borras E, Wilson DB, Valmori D, Simon R *et al.* A powerful combination: The use of positional scanning libraries and biometrical analysis to identify cross-reactive T cell epitopes. *Mol Immunol* 2004; **40**: 1063–1074.

[25] Ekeruche-Makinde J, Miles JJ, van den Berg HA, Skowera A, Cole DK, Dolton G *et al.* Peptide length determines the outcome of TCR/peptide-MHCI engagement. *Blood* 2013; **121**: 1112–1123.

[26] Varani S Landini MP. Cytomegalovirus-induced immunopathology and its clinical consequences. *Herpesviridae* 2011; **2:6**.

[27] Lossius A, Johansen JN, Vartdal F, Robins H, Šaltyte BJ, Holmøy T *et al.* High-throughput sequencing of TCR repertoires in multiple sclerosis reveals intrathecal enrichment of EBV-reactive $CD8^+$ T cells. *Eur J Immunol* 2014; **44**: 3439–3452.

[28] Skulina C, Schmidt S, Dornmair K, Babbe H, Roers A, Rajewsky K *et al.* Multiple sclerosis: brain-infiltrating $CD8^+$ T cells persist as clonal expansions in the cerebrospinal fluid and blood. *PNAS* 2004; **101**: 2428–2433.

[29] Burrows SR, Rossjohn J McCluskey J. Have we cut ourselves too short in mapping CTL epitopes? *Trends Immunol* 2006; **27**: 11–16.

[30] Sewell AK, Harcourt GC, Goulder PJ, Price DA Phillips RE. Antagonism of cytotoxic T lymphocyte-mediated

lysis by natural HIV-1 altered peptide ligands requires simultaneous presentation of agonist and antagonist peptides. *Eur J Immunol* 1997; **27**: 2323–2329.

[31] Price DA, Sewell AK, Dong T, Tan R, Goulder PJ, Rowland-Jones SL *et al.* Antigen-specific release of beta-chemokines by anti-HIV-1 cytotoxic T lymphocytes. *Curr Biol* 1998; **8**: 355–358.

[32] Wooldridge L, Laugel B, Ekeruche J, Clement M, van den Berg HA, Price DA *et al.* CD8 controls T cell cross-reactivity. *J Immunol* 2010; **185**: 4625–4632.

[33] Purbhoo MA, Li Y, Sutton DH, Brewer JE, Gostick E, Bossi G *et al.* The HLA A*0201-restricted hTERT(540-548) peptide is not detected on tumor cells by a CTL clone or a high-affinity T-cell receptor. *Mol Cancer Ther* 2007; **6**: 2081–2091.

[34] Ekeruche-Makinde J, Clement M, Cole DK, Edwards ES, Ladell K, Miles JJ *et al.* T-cell receptor-optimized peptide skewing of the T-cell repertoire can enhance antigen targeting. *J Biol Chem* 2012; **287**: 37269–37281.

[35] Price DA, Brenchley JM, Ruff LE, Betts MR, Hill BJ, Roederer M *et al.* Avidity for antigen shapes clonal dominance in $CD8^+$ T cell populations specific for persistent DNA viruses. *J Exp Med* 2005; **202**: 1349–1361.

[36] Phillips RE, Rowland-Jones S, Nixon DF, Gotch FM, Edwards JP, Ogunlesi AO *et al.* Human immunodeficiency virus genetic variation that can escape cytotoxic T cell recognition. *Nature* 1991; **354**: 453–459.

[37] Iglesias MC, Almeida JR, Fastenackels S, van Bockel DJ, Hashimoto M, Venturi V *et al.* Escape from highly effective public $CD8^+$ T-cell clonotypes by HIV. *Blood* 2011; **118**: 2138–2149.

[38] Chen H, Ndhlovu ZM, Liu D, Porter LC, Fang JW, Darko S *et al.* TCR clonotypes modulate the protective effect of HLA class I molecules in HIV-1 infection. *Nat Immunol* 2012; **13**: 691–700.

[39] Zhao Y, Gran B, Pinilla C, Markovic-Plese S, Hemmer B, Tzou A *et al.* Combinatorial peptide libraries and biometric score matrices permit the quantitative analysis of specific and degenerate interactions between clonotypic TCR and MHC peptide ligands. *J Immunol* 2001; **167**: 2130–2141.

[40] Rubio-Godoy V, Ayyoub M, Dutoit V, Servis C, Schink A, Rimoldi D *et al.* Combinatorial peptide library-based identification of peptide ligands for tumor-reactive cytolytic T lymphocytes of unknown specificity. *Eur J Immunol* 2002; **32**: 2292–2299.

[41] Clement M, Ladell K, Ekeruche-Makinde J, Miles JJ, Edwards ES, Dolton G *et al.* Anti-CD8 antibodies can trigger $CD8^+$ T cell effector function in the absence of TCR engagement and improve peptide-MHCI tetramer staining. *J Immunol* 2011; **187**: 654–663.

[42] Miles JJ, Borg NA, Brennan RM, Tynan FE, Kjer-Nielsen L, Silins SL *et al.* TCR alpha genes direct MHC restriction in the potent human T cell response to a class I-bound viral epitope. *J Immunol* 2006; **177**: 6804–6814.

[43] Tynan FE, Borg NA, Miles JJ, Beddoe T, El-Hassen D, Silins SL *et al.* High resolution structures of highly bulged viral epitopes bound to major histocompatibility complex class I. implications for T-cell receptor engagement and T-cell immunodominance. *J Biol Chem* 2005; **280**: 23900–23909.

[44] Goulder PJ, Sewell AK, Lalloo DG, Price DA, Whelan JA, Evans J *et al.* Patterns of immunodominance in HIV-1-specific cytotoxic T lymphocyte responses in two human histocompatibility leukocyte antigens (HLA)-identical siblings with HLA-A*0201 are influenced by epitope mutation. *J Exp Med* 1997; **185**: 1423–1433.

[45] Laugel B, van den Berg HA, Gostick E, Cole DK, Wooldridge L, Boulter J *et al.* Different T cell receptor affinity thresholds and CD8 coreceptor dependency govern cytotoxic T lymphocye activation and tetramer binding properties. *J Biol Chem* 2007; **282**: 23799–23810.

[46] Cole DK, Edwards ES, Wynn KK, Clement M, Miles JJ, Ladell K *et al.* Modification of MHC anchor residues generates heteroclitic peptides that alter TCR binding and T cell recognition. *J Immunol* 2010; **185**: 2600–2610.

[47] Wooldridge L, Lissina A, Vernazza J, Gostick E, Laugel B, Hutchinson SL *et al.* Enhanced immunogenicity of CTL antigens through mutation of the CD8 binding MHC class I invariant region. *Eur J Immunol* 2007; **37**: 1323–1333.

[48] Valitutti S, Müller S, Cella M, Padovan E Lanzavecchia A. Serial triggering of many T-cell receptors by a few peptide-MHC complexes. *Nature* 1995; **375**: 148 – 151.

[49] Valitutti S Lanzavecchia A. Serial triggering of TCRs: A basis for the sensitivity and specificity of antigen recognition. *Immunol Today* 1997; **18**: 299 – 304.

[50] van den Berg HA Rand DA. Quantitative theories of T-cell responsiveness. *Immunol Rev* 2007; **216**: 81–92.

Figure legends

Figure 1 Nonamer CPL scan of E7NLV:

6×10^4 C1R-A*0201 target cells were pulsed in duplicate with mixtures from a 9-mer CPL scan (100 μM) at 37°C. After 2 hours, 3×10^4 E7NLV CD8$^+$ T-cells were added and incubated overnight. The supernatant was then harvested and assayed for MIP1β by ELISA.

Figure 2 Recognition of 30 randomly chosen and uniformly distributed peptides by the E7NLV clone:

(a) 1×10^3 C1R-A*0201 target cells were pulsed with a panel of 30 peptides over a range of concentrations in duplicate for 1 hour at 37°C. 2×10^3 E7NLV CD8$^+$ T-cells were subsequently added at an E:T ratio of 2:1. Cytotoxic activity was measured via chromium release from target cells expressing C1R-A*0201 target cells as described in the Methods. **(b)** Relative functional sensitivity ($\Delta p\mathrm{EC}_{50}$) for the same 30 peptides compared to index ($\Delta p\mathrm{EC}_{50}=0$). (c) Scatter plot of $\Delta p\mathrm{EC}_{50}$ versus Λ for the same 30 peptides.

Figure 3 E7NLV recognition of the top six peptides (a) and peptides ranked 7-10 (b) from the human pathogen database: In (b), peptide recognition is compared to index (black upside-down triangle). Cytotoxic activity was measured via chromium release from target cells expressing HLA A*0201 as described in the Methods.

Figure 4 Heat maps summarizing CPL scan data for: E7NLV (a), SB16 (b), SB14 (c), SB27 (d), 003 (e), 868 (f), ILA1 (g) and MEL5 (h). CPL scan data are normalized in each row so that the values range from high (red) to low (blue); the maximum intensity is the largest of all red values in the rows. Amino acids are grouped according to

their physicochemical properties, as follows: polar, uncharged amines: Q, N; polar, uncharged alcohols: T, S; small: G, A, C; hydrophobic: A–H; aliphatic: V, I, L; aromatic: Y, F, W, H; large: F, W; charged basic: H, K, R; and charged acidic: E, D.

Figure 5 Three-stage strategy to dissect the peptide recognition signature of individual TCRs:

To augment community-wide access to CPL-driven database searching, we have created a dedicated webtool as part of the WSBC webtools framework.

Table for main text

Clone ID	Specificity	HLA Restriction	Minimal Epitope	Peptide Length	Reference
E7NLV	HCMV	A*0201	NLVPMVATV	9	*
SB16	EBV	A*0201	GLCTLVAML	9	*
SB12	EBV	A*0201	GLCTLVAML	9	*
ALF3	Influenza A	A*0201	GILGFVFTL	9	41
SB14	EBV	B*3508	HPVGEADYFEY	11	42
SBS27	EBV	B*3508	LPEPLPQGQLTAY	13	43
003	HIV-1	A*0201	SLYNTVATL	9	44
868	HIV-1	A*0201	SLYNTVATL	9	44
ILA1	Telomerase	A*0201	ILAKFLHWL	9	45
MEL5	Melan-A	A*0201	ELAGIGILTV	10	46

Table 1: $CD8^+$ T-cell clones used in this study.

* First description of this $CD8^+$ T-cell clone. The parental clone was used in all cases except for 868, where primary $CD8^+$ T-cells were transduced to express the 868 TCR.

Figure 1

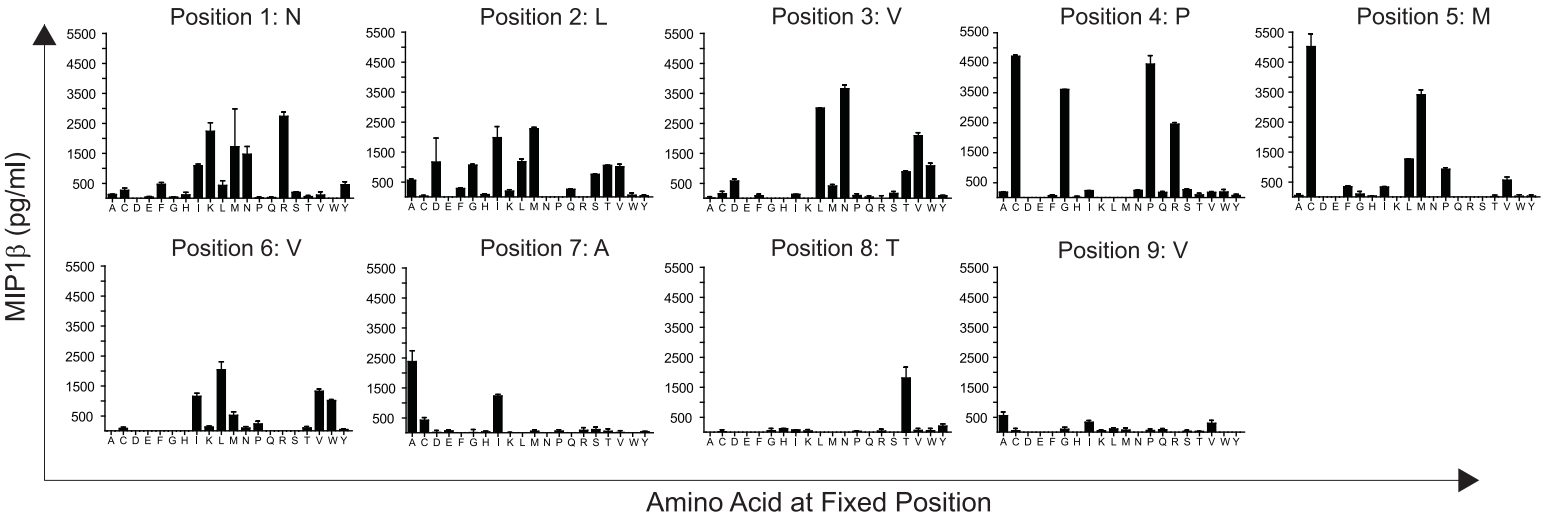
Position 1: N
Position 2: L
Position 3: V
Position 4: P
Position 5: M
Position 6: V
Position 7: A
Position 8: T
Position 9: V
5500
4500
3500
2500
1500
500
A C D E F G H I K L M N P Q R S T V W Y
MIP1β (pg/ml)
Amino Acid at Fixed Position

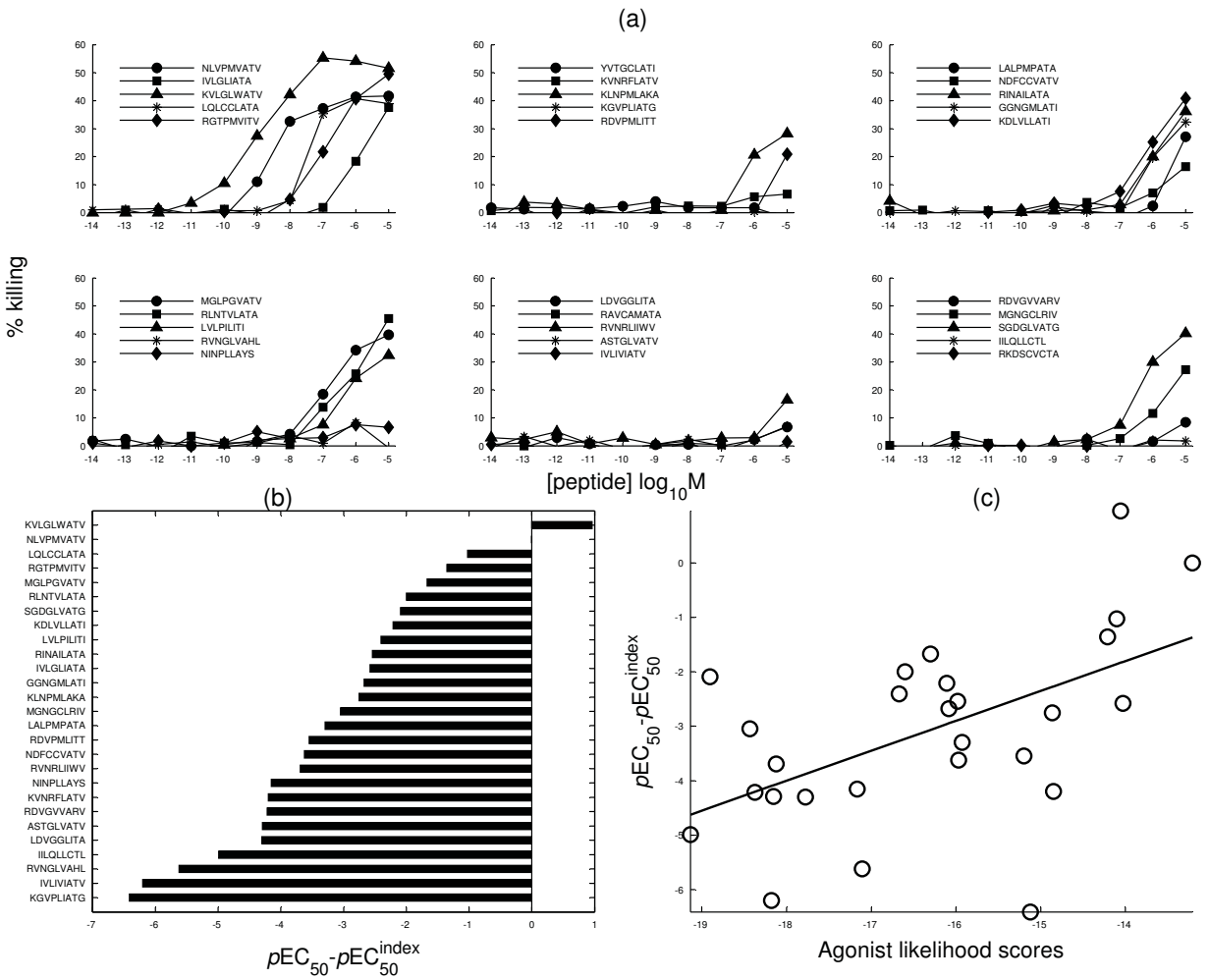
(a)
NLVPMVATV
IVLGLIATA
KVLGLWATV
LQLCCLATA
RGTPMVITV
YVTGCLATI
KVNRFLATV
KLNPMLAKA
KGVPLIATG
RDVPMLITT
LALPMPATA
NDFCCVATV
RINAILATA
GGNGMLATI
KDLVLLATI
MGLPGVATV
RLNTVLATA
LVLPILITI
RVNGLVAHL
NINPLLAYS
LDVGGLITA
RAVCAMATA
RVNRLIIWV
ASTGLVATV
IVLIVIATV
RDVGVVARV
MGNGCLRIV
SGDGLVATG
IILQLLCTL
RKDSCVCTA
% killing
[peptide] log10M
(b)
KVLGLWATV
NLVPMVATV
LQLCCLATA
RGTPMVITV
MGLPGVATV
RLNTVLATA
SGDGLVATG
KDLVLLATI
LVLPILITI
RINAILATA
IVLGLIATA
GGNGMLATI
KLNPMLAKA
MGNGCLRIV
LALPMPATA
RDVPMLITT
NDFCCVATV
RVNRLIIWV
NINPLLAYS
KVNRFLATV
RDVGVVARV
ASTGLVATV
LDVGGLITA
IILQLLCTL
RVNGLVAHL
IVLIVIATV
KGVPLIATG
pEC50-pEC50index
(c)
pEC50-pEC50index
Agonist likelihood scores

Figure 2

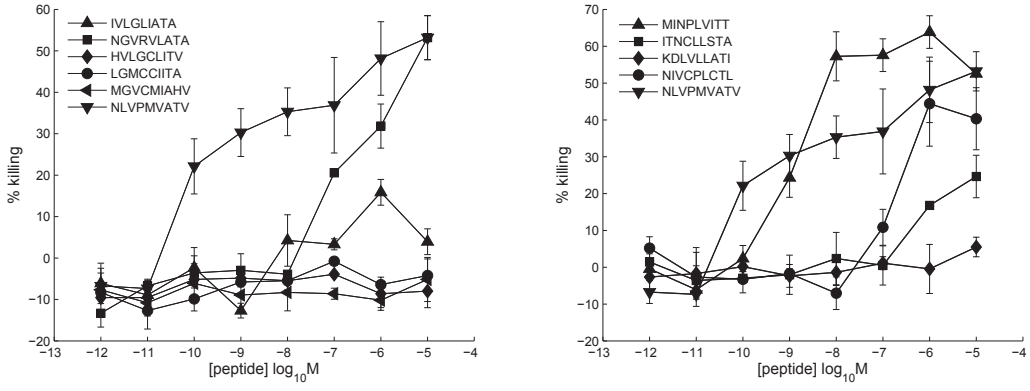
IVLGLIATA
NGVRVLATA
HVLGCLITV
LGMCCIITA
MGVCMIAHV
NLVPMVATV
% killing
[peptide] log10M
MINPLVITT
ITNCLLSTA
KDLVLLATI
NIVCPLCTL
NLVPMVATV
% killing
[peptide] log10M

(a) (b)

Figure 3:

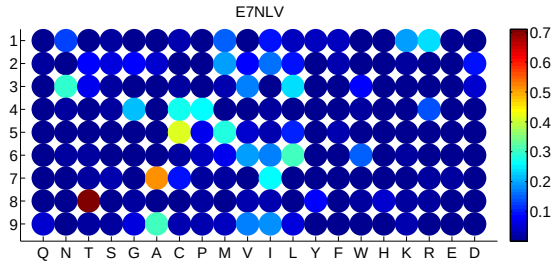

(a)

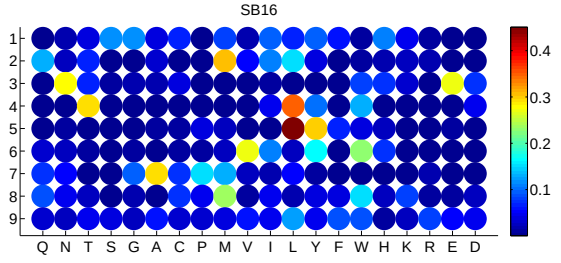

(b)

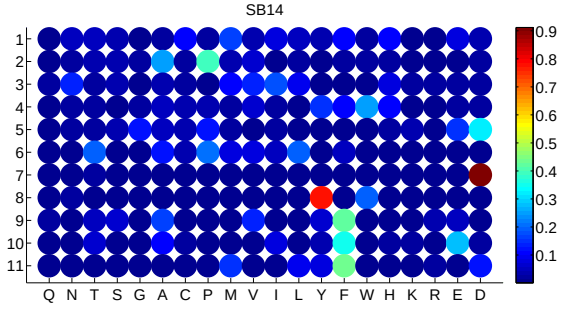

(c)

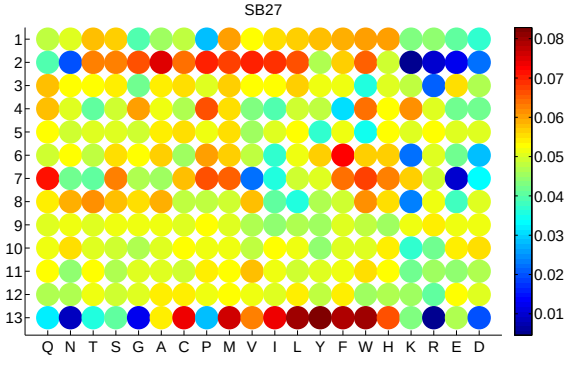

(d)

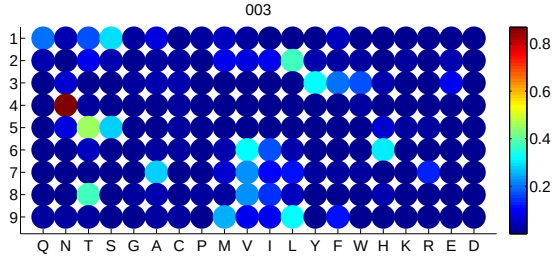

(e)

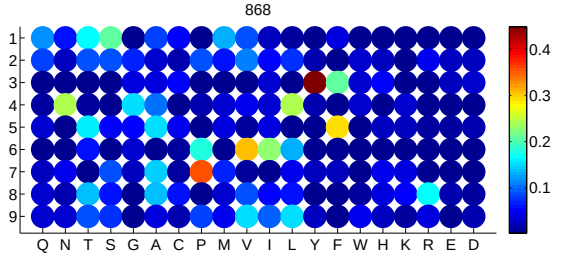

(f)

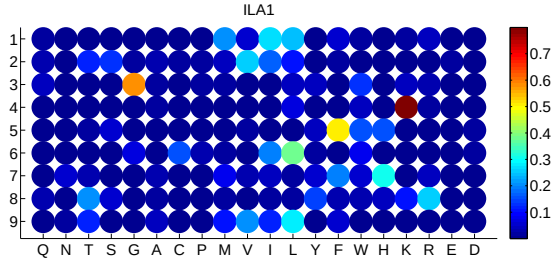

(g)

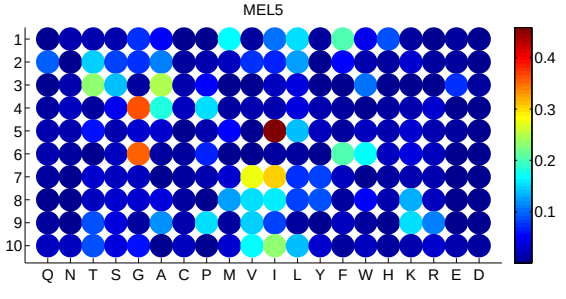

(h)

Figure 4:

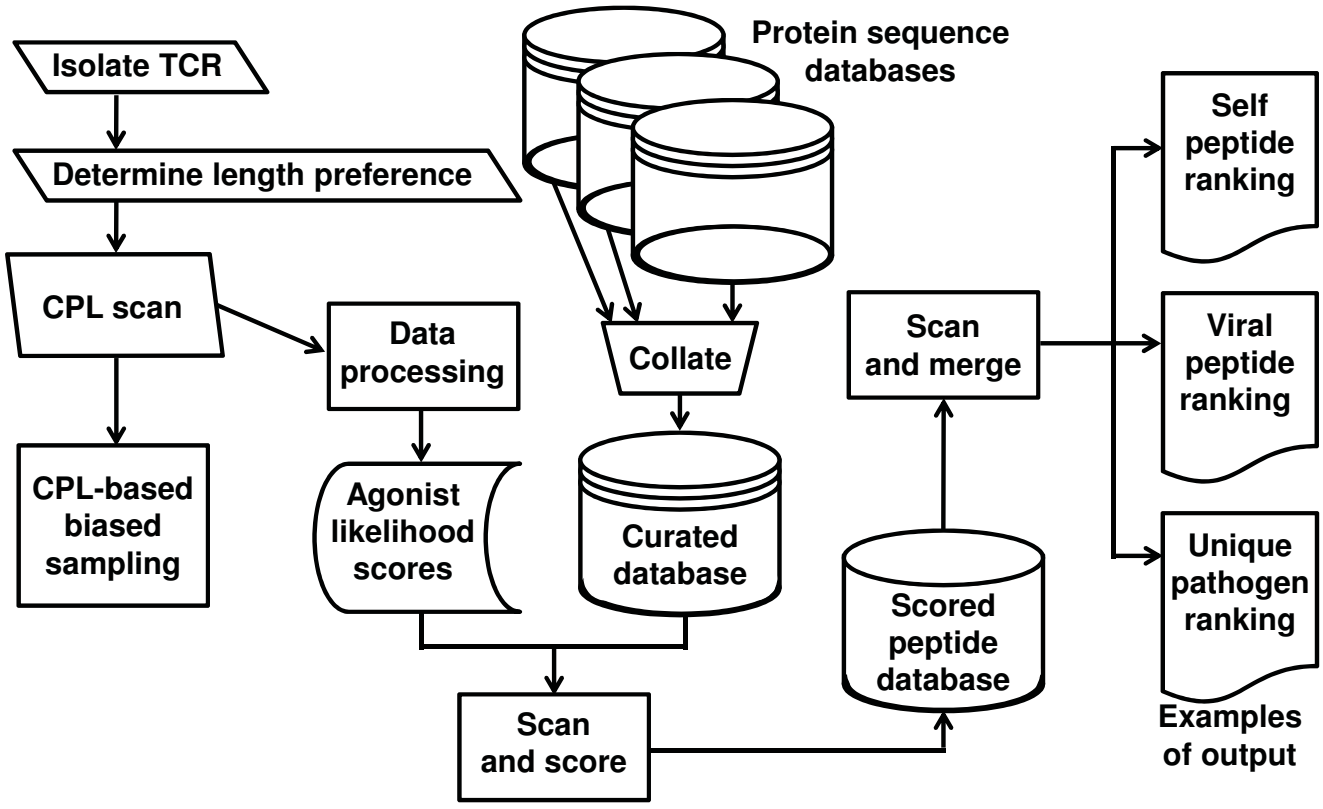
Isolate TCR
Determine length preference
CPL scan
CPL-based biased sampling
Data processing
Agonist likelihood scores
Protein sequence databases
Collate
Curated database
Scan and score
Scan and merge
Scored peptide database
Self peptide ranking
Viral peptide ranking
Unique pathogen ranking
Examples of output

Figure 5

Supplemental File

Identification of human viral protein-derived ligands recognized by individual major histocompatibility complex class I (MHCI)-restricted T-cell receptors

Barbara Szomolay, Jie Liu, Paul E. Brown, John J. Miles, Mathew Clement, Sian Llewellyn-Lacey, Garry Dolton, Julia Ekeruche-Makinde, Anya Lissina, Andrea J. Schauenburg, Andrew K. Sewell, Scott R. Burrows, Mario Roederer, David A. Price, Linda Wooldridge*, Hugo A. van den Berg*

Corresponding author: L. Wooldridge
Email: linda.wooldridge@bristol.ac.uk
*LW and HAB contributed equally to this manuscript.

SUPPLEMENTAL FIGURE LEGENDS

Figure S1: CPL scan of SB16 CD8$^+$ T-cells: 6x10^4 target cells expressing HLA A*0201 were pulsed in duplicate with mixtures from a 9-mer CPL scan (100 μM) at 37ºC. After 2 hours, 3x10^4 SB16 CD8$^+$ T-cells were added and incubated overnight. The supernatant was then harvested and assayed for MIP1β by ELISA.

Figure S2: CPL scan of SB12 CD8$^+$ T-cells: 6x10^4 target cells expressing HLA A*0201 were pulsed in duplicate with mixtures from a 9-mer CPL scan (100 μM) at 37ºC. After 2 hours, 3x10^4 SB12 CD8$^+$ T-cells were added and incubated overnight. The supernatant was then harvested and assayed for MIP1β by ELISA.

Figure S3: CPL scan of ALF3 CD8$^+$ T-cells: 6x10^4 target cells expressing HLA A*0201 were pulsed in duplicate with mixtures from a 9-mer CPL scan (100 μM) at 37ºC. After 2 hours, 3x10^4 ALF3 CD8$^+$ T-cells were added and incubated overnight. The supernatant was then harvested and assayed for MIP1β by ELISA.

Figure S4: CPL scan of SB14 CD8$^+$ T-cells: 6x10^4 target cells expressing HLA B*3508 were pulsed in duplicate with mixtures from an 11-mer CPL scan (100 μM) at 37ºC. After 2 hours, 3x10^4 SB14 CD8$^+$ T-cells were added and incubated overnight. The supernatant was then harvested and assayed for MIP1β by ELISA.

Figure S5: CPL scan of 003 CD8$^+$ T-cells: 6x10^4 target cells expressing HLA A*0201 were pulsed in duplicate with mixtures from a 9-mer CPL scan (100 μM) at 37ºC. After 2 hours, 3x10^4 003 CD8$^+$ T-cells were added and incubated overnight. The supernatant was then harvested and assayed for MIP1β by ELISA.

Figure S6: CPL scan of 868 CD8$^+$ T-cells: 6x10^4 target cells expressing HLA A*0201 were pulsed in duplicate with mixtures from a 9-mer CPL scan (100 μM) at 37ºC. After 2 hours, 3x10^4 CD8$^+$ T-cells transduced with the 868 TCR were added and incubated overnight. The supernatant was then harvested and assayed for MIP1β by ELISA.

Figure S1

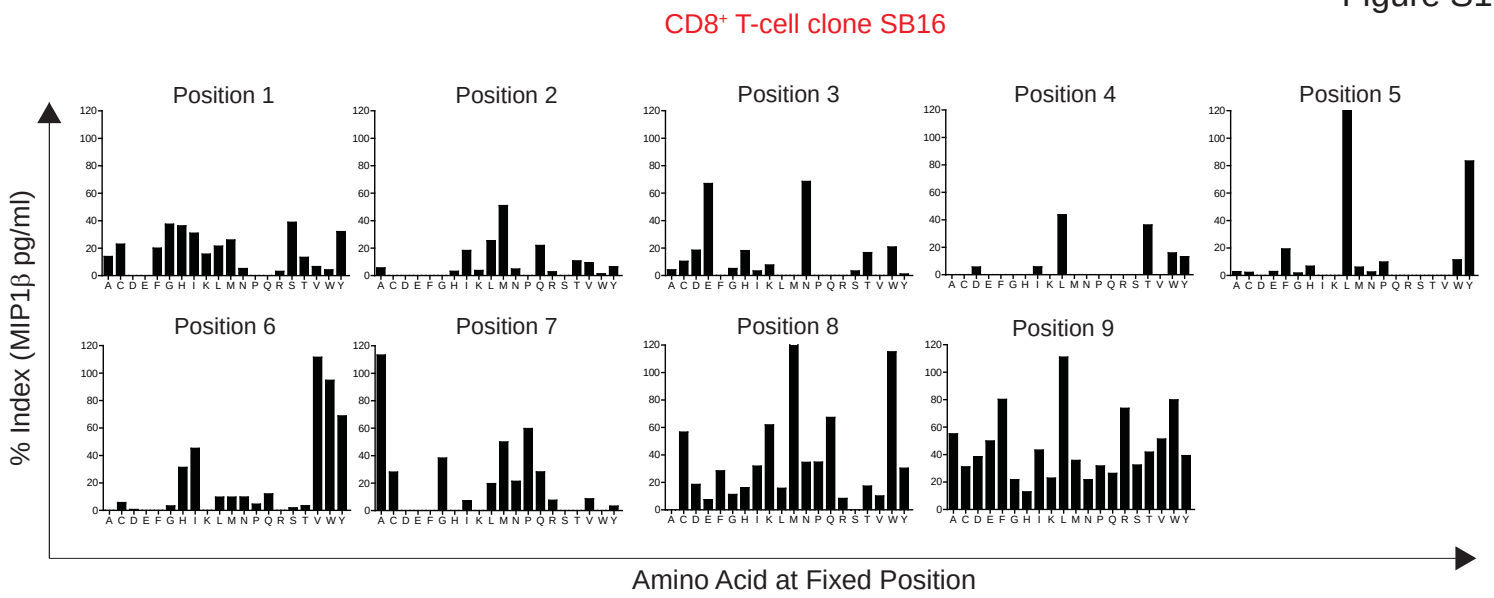
CD8+ T-cell clone SB16
Position 1
Position 2
Position 3
Position 4
Position 5
Position 6
Position 7
Position 8
Position 9
% Index (MIP1β pg/ml)
Amino Acid at Fixed Position

Figure S2

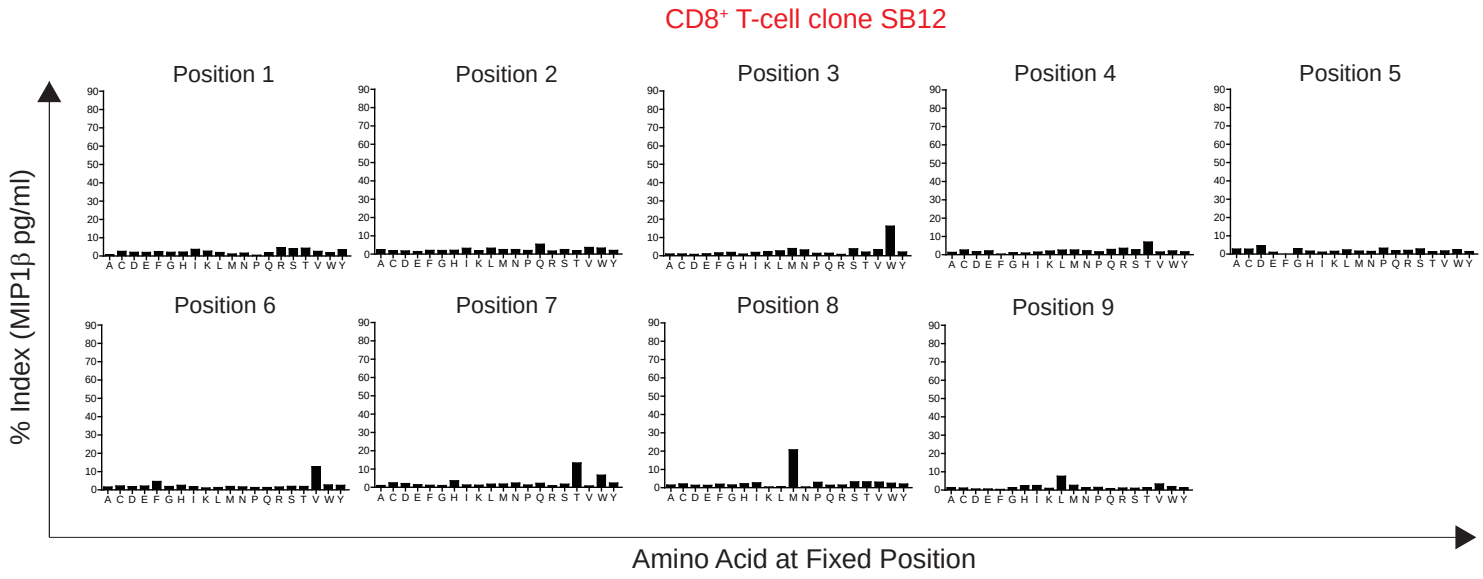
CD8+ T-cell clone SB12
Position 1
Position 2
Position 3
Position 4
Position 5
Position 6
Position 7
Position 8
Position 9
% Index (MIP1β pg/ml)
Amino Acid at Fixed Position

Figure S3

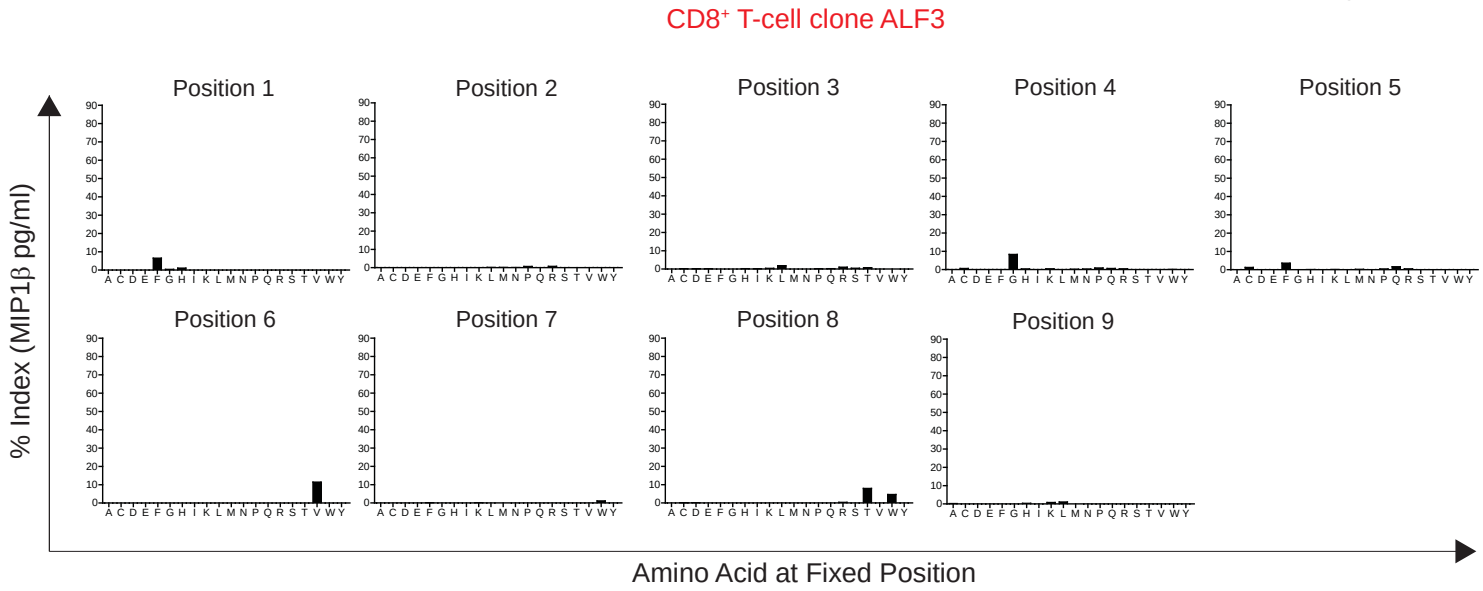
CD8+ T-cell clone ALF3
Position 1
Position 2
Position 3
Position 4
Position 5
Position 6
Position 7
Position 8
Position 9
% Index (MIP1β pg/ml)
Amino Acid at Fixed Position

Figure S4

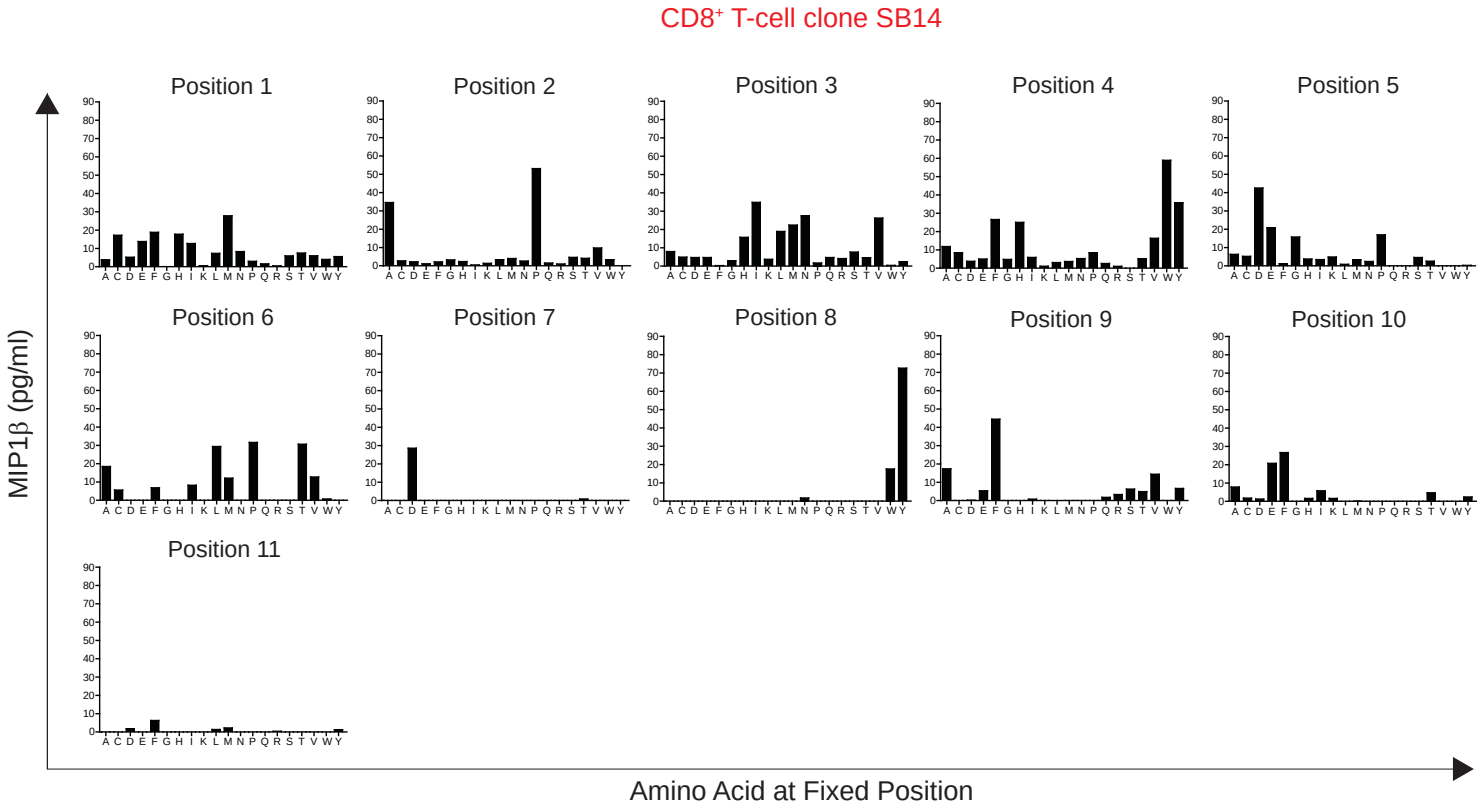
CD8+ T-cell clone SB14
Position 1
Position 2
Position 3
Position 4
Position 5
Position 6
Position 7
Position 8
Position 9
Position 10
Position 11
MIP1β (pg/ml)
Amino Acid at Fixed Position

Figure S5

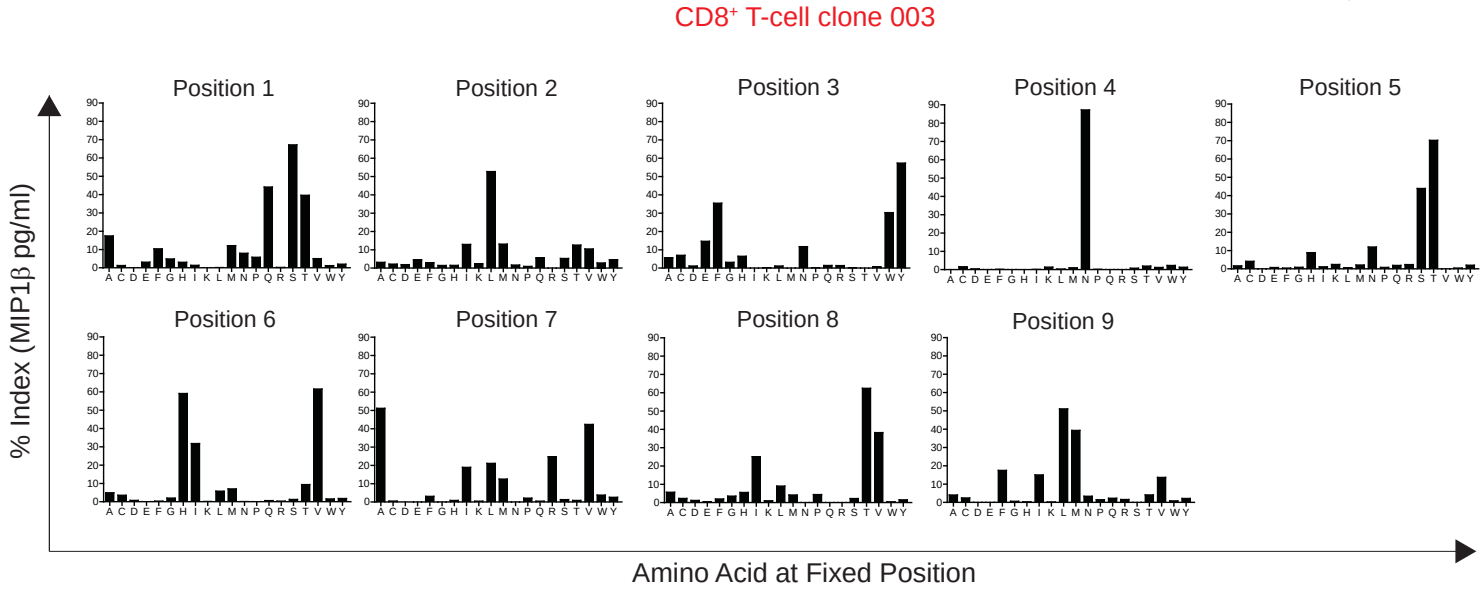
CD8+ T-cell clone 003
Position 1
Position 2
Position 3
Position 4
Position 5
Position 6
Position 7
Position 8
Position 9
% Index (MIP1β pg/ml)
Amino Acid at Fixed Position

Figure S6

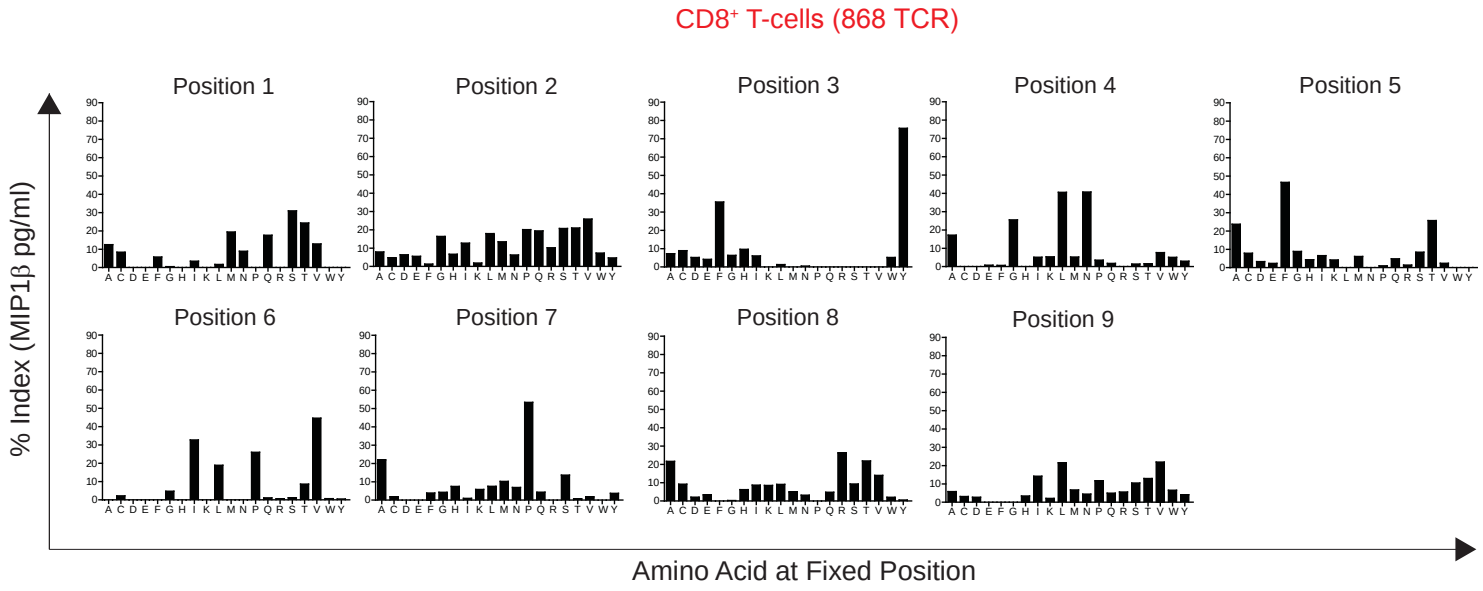
CD8+ T-cells (868 TCR)
Position 1
Position 2
Position 3
Position 4
Position 5
Position 6
Position 7
Position 8
Position 9
% Index (MIP1β pg/ml)
Amino Acid at Fixed Position

Supplementary Materials: Supplemental Tables

Rank	Λ	Peptide Sequence	Viral ID
1	**-13.21**	**NLVPMVATV**	**HUMAN CYTOMEGALOVIRUS**
2	-14.0927	IVLGLIATA	EASTERN EQUINE ENCEPHALITIS
3	-14.6606	NGVRVLATA	HUMAN METAPNEUMOVIRUS
4	-15.5807	HVLGCLITV	DENGUE VIRUS 2
5	-15.9006	LGMCCIITA	DENGUE VIRUS 2
6	-15.9495	MGVCMIAHV	HUMAN HERPESVIRUS 2
7	-15.9934	MINPLVITT	GUANARITO VIRUS
8	-16.0104	ITNCLLSTA	CRIMEAN-CONGO HEMORRHAGIC FEVER VIRUS
9	-16.1097	KDLVLLATI	HUMAN ADENOVIRUS B/D/E
10	-16.2304	NIVCPLCTL	HUMAN PAPILLOMAVIRUS 1A
11	-16.2601	MILGPISTA	MIDDELBURG VIRUS
12	-16.3254	IIVGCVPTI	HUMAN PAPILLOMAVIRUS 179
13	-16.52006	RLTGLLATS	HUMAN HERPESVIRUS 1
14	-16.5221	ILLACLATL	ALKHUMRA HEMORRHAGIC FEVER VIRUS
15	-16.5859	VVNPVVATA	HUMAN CYTOMEGLAOVIRUS
16	-16.5929	CMLRLVCTA	MOLLUSCUM CONTAGIOSUM VIRUS
17	-16.7047	KTNPLPATP	HUMAN HERPESVIRUS 1
18	-16.735	IVLRMVIYV	HUMAN IMMUNODEFICIENCY VIRUS 2
19	-16.779	MMLVPLITV	MONKEYPOX VIRUS
20	-16.8048	FILGIIITV	VARIOLA VIRUS

Table S1A: CPL-driven search of the human viral database for E7NLV (“Index” peptide sequence in boldface).

Rank	Λ	Peptide Sequence	Viral ID
1	**-15.3323**	**GLCTLVAML**	**HUMAN HERPESVIRUS 4**
2	-15.803	KMNTLVAQS	HUMAN TMEV-LIKE CARDIOVIRUS
3	-16.2656	SLNTLQPML	HUMAN PARAINFLUENZAVIRUS 1/3
4	-16.7366	LLEYLYMMR	TANAPOX VIRUS
5	-16.7367	GQNLLYANS	HUMAN ADENOVIRUS B/C
6	-16.7949	SLNLPVAKL	HUMAN IMMUNODEFICIENCY VIRUS 2
7	-16.8288	ILNTLVAYQ	HUMAN HERPESVIRUS 7
8	-16.9413	SLGLLVAWA	CERCOPITHECINE HERPESVIRUS 1
9	-17.0839	LLDTLVMQL	HUMAN HERPESVIRUS 8
10	-17.1431	LLELYVPKS	HUMAN HERPESVIRUS 7
11	-17.2793	TINTLIAMK	TANAPOX VIRUS
12	-17.3584	LYNLLVLWL	HUMAN HERPESVIRUS 6A
13	-17.3613	TLDTLVAMK	MOLLUSCUM CONTAGIOSUM VIRUS
14	-17.4863	ILWLLVMIF	HUMAN CORONAVIRUS Nl63
15	-17.5593	LQELLIQQW	SARS CORONAVIRUS
16	-17.5627	ILNLLVIQR	ISFAHAN VIRUS, CHANDIPURA VIRUS, VESICULAR STOMATITIS INDIANA VIRUS
17	-17.5649	NAELLVAME	INFLUENZA A VIRUS
18	-17.5647	SLNLPVAKV	HUMAN IMMUNODEFICIENCY VIRUS 1
19	-17.5699	TMDTLIAMK	MONKEYPOX VIRUS
20	-17.6729	TQELLYAYT	DHORI VIRUS

Table S1B: CPL-driven search of the human viral database for SB16 (“Index” peptide sequence in boldface).

Rank	Λ	Peptide Sequence	Viral ID
1	-17.2068	HPVAEADYFEY	HUMAN HERPESVIRUS 4
2	-17.3948	HPVGDADYFEY	HUMAN HERPESVIRUS 4
3	**-18.1085**	**HPVGEADYFEY**	**HUMAN HERPESVIRUS 4**
4	-20.203	SPQWAADYAFL	CERCOPITHECINE HERPESVIRUS 1
5	-20.3323	SPRWAADYAFL	CERCOPITHECINE HERPESVIRUS 16
6	-21.2014	FVNFNVDWVFF	HUMAN CORONAVIRUS NL63
7	-22.0733	LASLGVDYSEF	SUID HERPESVIRUS 1
8	-22.5825	TPNYDIDLAFF	HUMAN ADENOVIRUS B/E
9	-22.6401	YPNWDTIYYED	HUMAN PAPILLOMAVIRUS 167
10	-22.7321	LHAVPIDYFFL	ADULT DIARRHEAL ROTAVIRUS
11	-23.0102	PCMVGPDYAYF	MIDDLE EAST RESPIRATORY SYNDROME CORONAVIRUS
12	-23.0682	KNVWDVDYSAF	FOOT-AND-MOUTH DISEASE VIRUS
13	-23.1986	RNVWDVDYSAF	FOOT-AND-MOUTH DISEASE VIRUS
14	-23.3088	TGCCSTDYFEM	HUMAN CORONAVIRUS 229E
15	-23.5894	EVLREADYSED	ASTROVIRUS VA1
16	-23.5944	CLLLSTDWVEF	SAIMIRIINE HERPESVIRUS 2
17	-23.6211	DAIVEADYSAN	TIOMAN VIRUS
18	-23.7977	SVAPEVDWVAF	HUMAN CORONAVIRUS NL63
19	-23.9037	DAVVEADYSAN	MENANGLE VIRUS
20	-23.9122	PTSVPLDWAAF	HUMAN HERPESVIRUS 2

Table S1C: CPL-driven search of the human viral database for SB14 (“Index” peptide sequence in boldface).

Rank	Λ	Peptide Sequence	Viral ID
1	-34.9645	NVASLUGSTVREY	MOLLUSCUM CONTAGIOSUM VIRUS
2	-35.3404	LIENVASLUGSTV	MOLLUSCUM CONTAGIOSUM VIRUS
3	-35.6833	VASLUGSTVREYT	MOLLUSCUM CONTAGIOSUM VIRUS
4	-35.8699	SLUGSTVREYTQM	MOLLUSCUM CONTAGIOSUM VIRUS
5	-35.9034	ASLUGSTVREYTQ	MOLLUSCUM CONTAGIOSUM VIRUS
6	-36.0576	LLIENVASLUGST	MOLLUSCUM CONTAGIOSUM VIRUS
7	-36.481	VLLIENVASLUGS	MOLLUSCUM CONTAGIOSUM VIRUS
8	-36.6355	YLAPAPQTPLAFY	HUMAN HERPESVIRUS 2
9	-36.6396	APLPCFQNNCLFL	ENCEPHALOMYOCARDITIS VIRUS
10	-36.6518	SAAPAFQAPRFGL	WHATAROA VIRUS
11	-36.6783	HPFGSPQTDNPCY	TORQUE TENO VIRUS 19
12	**-36.7192**	**LPEPLPQGQLTAY**	**HUMAN HERPESVIRUS 4**
13	-36.7205	SAVKSPQAPLVLC	JUNIN ARENAVIRUS
14	-36.7216	LALPAPPSQPFPW	HUMAN T-LYMPHOTROPIC VIRUS 2
15	-36.7294	SAIKSPQAPLVLC	JUNIN VIRUS
16	-36.7331	WPEPTFPSRWYWL	HUMAN HERPESVIRUS 6A
17	-36.7375	WTLGLFQVSHGIF	HUMAN HERPESVIRUS 8
18	-36.7405	LLSPLPMTPEPTL	HUMAN HERPESVIRUS 6B
19	-36.7474	TVQGPFSAACGLF	HUMAN ADENOVIRUS A/F
20	-36.7475	TPMPPPQGPPTAM	HUMAN HERPESVIRUS 4

Table S1D: CPL-driven search of the human viral database for SB27 (“Index” peptide sequence in boldface).

Rank	Λ	Peptide Sequence	Viral ID
1	**-8.8549**	**SLYNTVATL**	**HUMAN IMMUNODEFICIENCY VIRUS 1**
2	-9.3363	SLFNTVATL	HUMAN IMMUNODEFICIENCY VIRUS 1
3	-9.3448	SLYNTVAVL	HUMAN IMMUNODEFICIENCY VIRUS 1
4	-9.8261	SLFNTVAVL	HUMAN IMMUNODEFICIENCY VIRUS 1
5	-10.006	SLYNTIAVL	HUMAN IMMUNODEFICIENCY VIRUS 1
6	-10.676	SLFNTIVVL	HUMAN IMMUNODEFICIENCY VIRUS 1
7	-11.038	SLHNTVATL	HUMAN IMMUNODEFICIENCY VIRUS 1
8	-12.608	SLYNAVATL	HUMAN IMMUNODEFICIENCY VIRUS 1
9	-13.286	SLYNAVVVL	HUMAN IMMUNODEFICIENCY VIRUS 1
10	-13.452	SLFNTTAIV	HUMAN IMMUNODEFICIENCY VIRUS 1
11	-14.216	SIDNTVATL	HUMAN PAPILLOMAVIRUS
12	-14.397	SLWNAIAVL	HUMAN IMMUNODEFICIENCY VIRUS 1
13	-14.531	TIFNTLLTL	ROTAVIRUS A
14	-14.586	SLWNAIVVL	HUMAN IMMUNODEFICIENCY VIRUS 1
15	-14.599	SMFNKVAVL	ROTAVIRUS A
16	-14.633	SLFNLVAVL	HUMAN IMMUNODEFICIENCY VIRUS 1
17	-14.669	SLGNTHVAM	HUMAN IMMUNODEFICIENCY VIRUS 1
18	-15.021	SMFNKVAIL	ROTAVIRUS A
19	-15.249	SLYNTVCVI	HUMAN IMMUNODEFICIENCY VIRUS 2
20	-15.335	QVYNTAIIL	YABA-LIKE DISEASE VIRUS

Table S1E: CPL-driven search of the human viral database for 003 (“Index” peptide sequence in boldface).

Rank	Λ	Peptide Sequence	Viral ID
1	**-15.1273**	**SLYNTVATL**	**HUMAN IMMUNODEFICIENCY VIRUS 1**
2	-15.2083	SLYNAVATL	HUMAN IMMUNODEFICIENCY VIRUS 1
3	-15.5765	SLYNTVAVL	HUMAN IMMUNODEFICIENCY VIRUS 1
4	-15.8067	SSYGAPPAP	SAPOVIRUS
5	-15.8858	SLYNTIAVL	HUMAN IMMUNODEFICIENCY VIRUS 1
6	-15.8864	SLFNTVATL	HUMAN IMMUNODEFICIENCY VIRUS 1
7	-16.3355	SLFNTVAVL	HUMAN IMMUNODEFICIENCY VIRUS 1
8	-16.4996	VLYNFVSTP	SAIMIRIINE HERPESVIRUS 2
9	-16.5179	SLYNALAVL	HUMAN IMMUNODEFICIENCY VIRUS 1
10	-16.7137	ASYGAPPAP	SAPOVIRUS
11	-16.9083	TTFAAVAAV	COXSACKIEVIRUS A24
12	-16.957	SVYNFLSKT	MONKEYPOX VIRUS, VACCINIA VIRUS, VARIOLA VIRUS
13	-17.0372	SIFNIVPRT	MONKEYPOX VIRUS, VACCINIA VIRUS, VARIOLA VIRUS
14	-17.1894	SLHNTVATL	HUMAN IMMUNODEFICIENCY VIRUS 1
15	-17.2614	TGYYAVPTV	HUMAN HERPESVIRUS 6A
16	-17.3227	SNYLQPPRL	HUMAN HERPESVIRUS 3
17	-17.4171	AMYNSVPLV	CRIMEAN-CONGO HEMORRHAGIC FEVER VIRUS
18	-17.4273	TGYNFPHKL	HUMAN PAPILLOMAVIRUS
19	-17.4426	TTYLALMAT	DENGUE VIRUS 1
20	-17.496	TPYNFIAKN	VACCINIA VIRUS

Table S1F: CPL-driven search of the human viral database for 868 (“Index” peptide sequence in bold face).

Rank	Λ	Peptide Sequence	Human Self Protein ID
1	-13.8709	LSGKWLMHL	UPF0696 protein C11orf68
2	-14.6509	LTQKWCHTL	F-box/LRR-repeat protein 6
3	-14.7419	LLGKFCTTF	cubilin precursor
4	-14.9425	IILKFLARI	semaphorin-6A
5	-14.9697	LLGLFLFQL	semaphorin-4A
6	-15.006	MTGKFCIIL	olfactory receptor 11H6
7	-15.1703	IIGKFCTAL	phospholipase A1 member A
8	**-15.2091**	**ILAKFLHWL**	**telomerase reverse transcriptase**
9	-15.3153	LTGAFLFSL	ATP-sensitive inward rectifier potassium channel 10/15
10	-15.4063	LQGLFLFSL	dynein heavy chain 3, axonemal
11	-15.4983	NIGKFLNRI	protein strawberry notch homolog
12	-15.5045	IIGKFQFTV	protein-glutamine gamma-glutamyltransferase K
13	-15.5077	ITRKHLWRL	coiled-coil domain-containing protein 108
14	-15.5221	MVGKFGVTA	Solute carrier family 22
15	-15.54	MSGWFLRRT	Putative DNA repair and recombination protein RAD26
16	-15.5526	ILGKHGFFV	phosphoglucomutase-1
17	-15.5801	FLGKSLFSL	epidermal retinol dehydrogenase 2
18	-15.6492	MLGLFLYSL	otoferlin
19	-15.6538	MTGLWIFTI	N-formyl peptide receptor 3
20	-15.7099	LIQKHLVRL	E3 ubiquitin-protein ligase UBR1

Table S2A: CPL-driven search of the human self database for ILA1 (“Index” peptide sequence in boldface).

Rank	Λ	Peptide Sequence	Human Self Protein ID
1	-16.8944	LLAGIGTVPI	solute carrier organic anion transporter
2	-17.418	ILEGIGILAV	anoctamin-3
3	-17.5337	LLLGIGILVL	bone marrow stromal antigen 2
4	-17.6102	FLAGLGLLVI	translocon-associated protein subunit alpha
5	-17.6562	AAAAIFVIII	MHC class I polypeptide-related sequence A
6	-17.7312	FVAGIFLLVV	protocadherin Fat 1 precursor
7	-17.9409	FITGKGIVAI	leiomodin-3
8	-18.0041	LITGLGIISV	adenosine receptor A3
9	-18.013	ILLGIGIYAL	transmembrane and coiled-coil domain-containing protein 2
10	-18.0426	LLAGLGILAG	provirus ancestral Env polyprotein preproprotein
11	-18.1265	ISAAIWIVVG	putative P2Y purinoceptor 10
12	-18.1456	IAAGTGIVIL	transmembrane 7 superfamily member 4
13	-18.228	FITATGVVKL	serine/threonine-protein kinase Nek6
14	-18.2536	ITAGLPVKVV	amyloid protein-binding protein 2
15	-18.2816	LKTGIGVIRM	neuropilin and tolloid-like protein 2 precursor
16	-18.3184	SLTGLGVVKV	E3 ubiquitin-protein ligase HERC2
17	-18.3348	WTAPIGVISL	uncharacterized protein C5orf4
18	-18.3916	FITGTGILAL	tropomodulin-2
19	-18.399	AGTGIGLMVL	intermediate conductance calcium-activated potassium channel protein 4
20	-18.4265	ILEGIGILSV	anoctamin-4

Table S2B: CPL-driven search of the human self database for MEL5 (EAAGIGILTV ranked 55).